

Close-Proximity Flight Validation Analysis with FlightStream®

By

Taylor Wayne Owens

A thesis submitted to the Graduate Faculty of
Auburn University
in partial fulfillment of the
requirements for the Degree of
Master of Science

Auburn, Alabama
August 3, 2019

Keywords: Unstructured Mesh, Aerodynamic Loads, FlightStream®

Copyright 2019 by Taylor Wayne Owens

Approved by

Dr. Roy Hartfield, Chair, Woltosz Professor, Department of Aerospace Engineering
Dr. Joseph Majdalani, Francis Chair, Department of Aerospace Engineering
Dr. John Cochran, Professor Emeritus, Department of Aerospace Engineering

Abstract

The objective of this research is to validate the use of FlightStream® in accurately predicting aerodynamic loads in a scenario of close-proximity flight, such as an aerial refueling and formation flight environment. The research will include individually validating wind tunnel data of each the KC-135 Stratotanker and the ICE-101 Configuration UAV. Once that is accomplished and model accuracy achieved, a formation flight and aerial refueling analysis will be conducted to validate FlightStream's capabilities as a computational solver. Models of both the KC-135 and the UAV were generated using NASA Open Vehicle Sketch Pad and exported as .STL files into FlightStream®. This thesis will show the utility of FlightStream's capability of providing a high-fidelity solution with less user inputs, than that of Computational Fluid Dynamics or other computational methods.

Acknowledgments

The author would like to thank Dr. Roy Hartfield for the opportunity, continuous support, and availability throughout the process of conducting this research. Thanks, are also due to Dr. John Cochran and Dr. Joseph Majdalani, for their assistance and encouragement when reviewing my work and answering questions. Also, thanks to Dr. Vivek Ahuja for developing FlightStream® to make this topic possible, providing tutorial sessions, as well as answering any questions that arose. Finally, many thanks are due to my parents, Mark and Dana Owens, for their constant support and encouragement throughout all my endeavors. None of this could have been accomplished without them.

Style manual or journal used:

American Institute of Aeronautics and Astronautics Journal

Computer software used:

FlightStream®, NASA Open Vehicle Sketch Pad

Table of Contents

Abstract	ii
Acknowledgements	iii
Style Manual	iv
Table of Contents	v
List of Illustrations	ix
List of Tables	xi
Appendix.....	xii
Nomenclature	xiii
1. Introduction.....	1
1.1 Motivation	
1.2 Thesis Synopsis	
2. Environments and Aircrafts	4
2.1 Close-Proximity Flight Environments	
2.1.1 Formation Flight.....	
2.1.2 Aerial Refuel	
2.2 Aircrafts.....	
2.2.1 Boeing KC-135 Stratotanker	
2.2.2 ICE-101 Configuration UAV	
3. Computational Testing Methods.....	10
3.1 Traditional Methods	
3.1.1 Introduction	

3.1.2 Empirical Formulation.....	
3.1.3 Potential Flow Methods.....	
3.1.4 Computational Fluid Dynamics.....	
3.1.5 Experimental Test Flights.....	
3.2 FlightStream®.....	
3.2.1 Introduction	
3.2.2 Integration and Meshing.....	
3.2.3 Solutions.....	
3.2.4 Synopsis.....	
4. Wind Tunnel Tests.....	18
4.1 Boeing KC-135 Stratotanker Case Study.....	
4.1.1 Introduction	
4.1.2 Wind Tunnel Setup.....	
4.1.3 Results	
4.2 ICE-101 Configuration UAV Case Study.....	
4.2.1 Introduction	
4.2.2 Wind Tunnel Setup.....	
4.2.3 Results	
4.3 UAV Formation Flight Case Study.....	
4.3.1 Wind Tunnel Setup.....	
4.3.2 Results	
4.4 Aerial Refueling Case Study.....	
4.4.1 Introduction	

4.4.2 Wind Tunnel Setup.....	
4.4.3 Results	
5. FlightStream® Analysis.....	30
5.1 NASA Vehicle Sketch Pad.....	
5.1.1 Introduction	
5.1.2 Integration and Meshing.....	
5.1.3 Boeing KC-135 Stratotanker Model Geometry.....	
5.1.4 ICE-101 UAV Configuration Model Geometry.....	
5.2 FlightStream® Results	
5.2.1 Introduction	
5.2.2 ICE-101 UAV Configuration Validation Study.....	
5.2.3 UAV Formation Flight Validation Study.....	
5.2.4 Boeing KC-135 Stratotanker Validation Study.....	
5.2.5 Aerial Refueling Validation Study.....	
6. Concluding Remarks.....	46
6.1 Conclusion to Validation Analysis.....	
6.2 Future Work	
6.2.1 FlightStream® Updates	
6.2.1 Commercial Sector.....	
6.2.2 Boeing KC-46 Aerial Refueling Analysis.....	
Appendix 1: Boeing KC-135 Aerodynamic Loads.....	49
Appendix 2: ICE-101 Configuration UAV Aerodynamic Loads	58
Appendix 3: UAV Formation Flight Aerodynamic Loads	68

Appendix 4: Aerial Refueling Aerodynamic Loads	75
References.....	87

List of Illustrations

Figure 2.1: F-35A Formation Flight	5
Figure 2.2: Aerial Refuel	6
Figure 2.3: Probe-and-Drogue	7
Figure 2.4: Flying Boom.....	8
Figure 2.5: Boeing KC-135 Stratotanker	8
Figure 2.6 ICE-101 Configuration UAV	9
Figure 3.1: Method of Analysis Comparison.....	14
Figure 3.2: FlightStream® Workflow.....	16
Figure 4.1: Boeing KC-135 3-View Schematic	19
Figure 4.2: KC-135 Coefficient of Lift vs. AOA.....	20
Figure 4.3: ICE-101 Configuration UAV 3-View Schematic	21
Figure 4.4: ICE-101 Configuration UAV Control Surfaces	22
Figure 4.5: Individual UAV Coefficient of Lift vs. AOA	23
Figure 4.6: Wind Tunnel Formation Flight Setup	24
Figure 4.7: Vertical, Lateral, and Longitudinal Spacing	24
Figure 4.8: Formation Flight Coefficient of Lift vs. Lateral Spacing.....	25
Figure 4.9: Trail Aircraft AOA 0 Results	25
Figure 4.10: Aircraft Model Comparison	27
Figure 4.11: Aerial Refueling Wind Tunnel Results	29
Figure 5.1: Boeing KC-135 Airfoil Location	32
Figure 5.2: Boeing KC-135 Airfoils	33

Figure 5.3: Boeing KC-135 Left View	33
Figure 5.4: Boeing KC-135 Top View	33
Figure 5.5: Boeing KC-135 Front View	34
Figure 5.6: Boeing KC-135 Left ISO View	34
Figure 5.7: Boeing KC-135 Left View without Inlets	34
Figure 5.8: Boeing KC-135 Top View without Inlets	35
Figure 5.9: Boeing KC-135 Front View without Inlets	35
Figure 5.10: Boeing KC-135 Left ISO View without Inlets.....	35
Figure 5.11: Boeing KC-135 CompGeom View	36
Figure 5.12: Boeing KC-135 CompGeom View without Inlets	36
Figure 5.13: ICE-101 Configuration UAV Left View.....	37
Figure 5.14: ICE-101 Configuration UAV Top View	37
Figure 5.15: ICE-101 Configuration UAV Front View.....	38
Figure 5.16: ICE-101 Configuration UAV Left ISO View	38
Figure 5.17: ICE-101 Configuration UAV CompGeom View.....	38
Figure 5.18: ICE-101 Configuration UAV FlightStream® Analysis	40
Figure 5.19: Formation Flight FlightStream® Analysis.....	41
Figure 5.20: Boeing KC-135 0.035 FlightStream® Analysis	43
Figure 5.21: Boeing KC-135 0.077 FlightStream® Analysis.....	44
Figure 5.22: Aerial Refueling FlightStream® Analysis	45

List of Tables

Table 3.1: Method of Analysis	11
Table 4.1: Boeing KC-135 Characteristics	19
Table 4.2: ICE-101 Configuration UAV Characteristics	22
Table 4.3: Boeing KC-135 0.077 Characteristics	27

Appendices

Appendix 1: Boeing KC-135 Aerodynamic Loads.....	49
Appendix 2: ICE-101 Configuration UAV Aerodynamic Loads	58
Appendix 3: UAV Formation Flight Aerodynamic Loads	68
Appendix 4: Aerial Refueling Aerodynamic Loads	75

Nomenclature

.IGES	Initial Graphics Exchange Specification
.STL	Stereolithography
AFRL	Air Force Research Labs
AMT	All Moving Tip
AOA	Angle of Attack
CAD	Computer Aided Design
CFD	Computational Fluid Dynamics
C_L	Coefficient of Lift
HASC	High Angle of Attack Stability and Control
ICE	Innovative Control Effector
KC-135	Boeing KC-135 Stratotanker
LFST	Langley Full-Scale Tunnel
LS	Lateral Spacing
MAC	Mean Aerodynamic Chord
MPH	Miles per Hour
NACA	National Advisory Committee for Aeronautics
NASA	National Aeronautics and Space Administration
NATO	North Atlantic Treaty Organization
NPSS	Numerical Propulsion System Simulation
SSD	Spoiler Slot Deflector
UAV	Unmanned Aerial Vehicle

UCAV Unmanned Combat Aerial Vehicle

USAF United States Air Force

VSP Vehicle Sketch Pad

Chapter 1

Introduction

1.1 Motivation

This work is fueled by the desire and requirement to better understand and optimize the aerodynamics of aircraft under varying in-flight scenarios in order to enhance safety and increase in-air capabilities. This progress expands the usefulness and versatility of air travel and military operations. Proximity flight in particular adds an additional element of complexity to the already challenging problem of flight, and is of utmost importance to refueling, urban flight, acrobatics, and many other applications.

Both experimental and analytic methods have been developed to test aircraft and flight characteristics for proximity flight. This work focuses on the challenging problem of developing analytic tools which are capable of predicting loads during proximity flight efficiently and reliably during conceptual and preliminary design, where the design can still be affected by aerodynamic analysis. Clearly some methods produce higher fidelity solutions than others. The general rule is that the higher fidelity solutions require the longest run times. This work focuses on a method which seeks the area of the pareto front which minimizes both analysis time and loss of fidelity.

To date, an inherent limitation of conceptual design has been the lack of an efficient computational solver that can produce a high-fidelity solution. While there are robust solvers, such approaches are not typically practical for early design in a sense of time and computational hardware requirements. Specifically, volume based Navier-Stokes numerical solutions typically require extensive learning curves, due to user inputs, or require a large amount of computational

power to run enough iterations to produce significant results. This problem increases in a more complex testing environment, such as a close-proximity flight. Proximity flying includes crowded environments an aircraft flies in, air-to-air refueling, formation flights, aircraft carrier landings and departures, urban flight near tall structures, indoor flight and many other applications of contemporary interest. For the classic refueling problem, the additional geometry inputs and the needed detail in the trailing wake of a lead aircraft makes these scenarios more difficult to predict or test. The scale of the problem is dramatically increased adding geometrically to the computational resources required to simulate the problem with a volumetric numerical solution.¹

For problems in which the primary consideration is the aerodynamic loads, moments and aggregate field variable distribution, quasi-potential theory approaches can dramatically reduce the computation resources required for an accurate design-integrated aerodynamic analysis. FlightStream® is a leading tool in this area. FlightStream® is primarily a surface-vorticity flow solver and has been developed to work seamlessly with modern engineering workflows. By incorporating state of the art models for viscous effects, FlightStream® is capable of reliably modeling loads and moments for a full range of aircraft and flight conditions required for design. Vortex-based solvers are known for their robustness, while being capable of running an analysis very efficiently. Legacy vorticity-based approaches, such as vortex lattice methods, and vortex paneling approaches, such as VSAero, are generally limited to linear (potential) solutions on specialized structured grids. FlightStream® incorporates many non-linear aerodynamic effects and runs on a variety of meshes including fully unstructured grids. As a result, FlightStream® remains a low order, but relatively high-fidelity solver¹. This thesis will validate FlightStream's robustness for predicting aerodynamic loads in a close-proximity environment.

1.2 Thesis Synopsis

Formation flight and aerial refueling scenarios are the focus of this work. FlightStream® solutions for such conditions are developed and compared to wind tunnel data by using the advantages of potential flow theory to solve for loads involving multiple aircraft in a confined environment simultaneously.

The motivating factors for conducting this research are reviewed in Chapter 1 and emphasized throughout it. A review of the types of environments, maneuvers, and aircraft researched will be established in Chapter 2. The current aircraft optimization and design process are described in Chapter 3 along with the role of FlightStream® in this process. Chapter 4 described multiple wind tunnel tests referenced to validate the approach. Chapter 5 presented FlightStream®, including the solver inputs, initialization, and testing results. Concluding remarks and comments on future work and the future possibilities of aerial refueling comprise Chapter 6.

Chapter 2

Environments and Aircrafts

2.1 Close-Proximity Flight Environments

2.1.1 Formation Flight

Formation flight can be used to conserve fuel for the trailing aircraft through drag reduction. The decrease in induced drag is caused by the upwash formed by the vortex system of a lifting wing. Basically, in a formation flight the rear aircraft becomes an extension of the span of the leading aircraft, which would be similar to increasing the aspect ratio.² Research in this area has included a wide range of wind tunnel and flight test including NASA studies with multiple F-18A aircraft flying in a “V-Pattern” and is seen elsewhere, such as nature with birds flying in a similar pattern. Figure 2.1 shows an example of this Flying V pattern, which is a type of formation flight. NASA has a charge to work on technologies, which will decrease fuel burn. This ongoing struggle will keep research in to this this type of flying maneuver relevant, and will encourage further research in drag reduction associated with this approach. Research into the potential fuel savings of proximity flight spawn the increased need to study the safety related issues as well. It is a complex environment that needs to be carefully executed to reach its full potential.²



Figure 2.1: F-35A Formation Flight³

2.1.2 Aerial Refuel

The military uses aerial refueling to increase the range of its aircraft. Air-to-air refueling, as illustrated in Figure 2.2, allows for the opportunity to reduce the need for forward basing requirements, decrease response times for critical targets, and increase loiter times for surveillance aircraft. Along with longer flight comes the capability of carrying heavier payloads. The aircraft can meet its takeoff weight with less fuel and more payload, then once in the air, refuel and extend its flight time tremendously than it would normally be with that weight.^{4,5} The military benefits are known, and with the continued improvements in aircraft design and safety, the civilian use could also potentially lead to optimized practices. Currently, refueling autonomous vehicles is a desirable scenario to incorporate into missions to increase the military's capabilities in more dangerous environments and for the increased safety and use of carrying bomb loads.⁴ Not only is it beneficial logistically, but it also saves fuel and time from having to land, refuel, and takeoff again to complete especially station keeping missions. It is estimated by not having to go through this landing and takeoff procedure, longer distance flights result in a fuel savings of up to 35-40 percent for the receiving vehicle.^{4,5}

A fast aerodynamic solver is required to investigate the multi-dimensional problem of optimizing fuel burn and exploring the safety related issues of the aerial refueling process. These are complex environments that lower order solvers cannot typically accurately predict because of the level of detail required to represent the scenario. To provide an accurate analysis, there has to be time to allow for the consideration of a substantial number of design alternatives and runs. An efficient conceptual and preliminary design tool for a multi-dimensional problem must become more robust to shorten the cycle time²⁸. To explore the fundamentals of analyzing the aerodynamics of refueling based proximity flights using a vorticity-based solver, this thesis focuses on a well-documented refueling effort of a KC-135 and an Unmanned Aerial Vehicle (UAV).



Figure 2.2: Aerial Refuel⁶

The process of transferring fuel from one aircraft to another is done with two main systems on board, the probe-and-drogue or the flying boom. The probe-and-drogue, illustrated in Figure 2.3, is the simplest method by attaching the parts to an existing aircraft. A flexible hose trails from the tanker aircraft to the receiver, and a drogue stabilizes the hose mid-flight to provide a funnel to the hose drum unit. The receiving aircraft has a probe unit attached to it to

complete the connection. In this situation all parts used on each aircraft are typically designed to be fully retractable⁴. The flying boom, shown in Figure 2.4, is a rigid, telescope-like tube with movable flight control surfaces. This method requires a complex modification to an existing aircraft configuration, as well as an operator on the tanker to extend it and insert it into a receptacle on the receiver. While more complex, it is often used for its ability to have high fuel flow rates, and less susceptible to pilot error on the receiving aircraft due to the additional operator. It is also more durable in adverse weather conditions that would generally greatly inhibit the other option.^{4,5} The Air Force's fixed-wing program primarily uses the flying boom method, while Air Force helicopters, all Navy and Marine Corps aircraft, NATO countries, and other allies use the hose-and-drogue method.⁷ Here, the KC-135 uses a flying boom while refueling a UAV.



Figure 2.3: Probe-and-Drogue⁸



Figure 2.4: Flying Boom⁸

2.2 Aircrafts

2.2.1 Boeing KC-135 Stratotanker

A tanker fleet is essential for the combat portion of the fleet to get into and maintain engagement in military operations.⁹ The Boeing KC-135 Stratotanker, created from the Boeing 707 airframe, is a tanker designed to provide fuel to a receiving aircraft. Entering service in 1957, it is the Air Force's first jet-powered refueling tanker. It fits elite company as one of six military fixed-wing aircraft with 50 years of continuous service.¹⁰⁻¹³ Figure 2.5 illustrates a KC-135 in flight.



Figure 2.5: Boeing KC-135 Stratotanker¹⁴

2.2.2 ICE-101 Configuration UAV

Contemporary UAVs perform a range of military critical missions including beyond-human-endurance requirements, keeping service personnel out of harm's way, surveillance, and flight during uninhabitable conditions.¹⁵

The Innovative Control Effectors (ICE) program was conducted by the AFRL and Lockheed Martin to create a conceptual fighter airplane for future strike missions. The ICE vehicle was designed as an agile fighter aircraft, with low observability features, and a tailless design to fly at up to a high angle of attack.¹⁶ The research interest in designing it was with the goal of investigating innovative aerodynamic control concepts for highly maneuverable, tailless fighters.¹⁷ These control surfaces include pitch flaps, ailerons, leading-edge flaps, SSDs, and AMTs.¹⁸ ICE has similar aerodynamic characteristics to a standard 65-degree delta wing, but with a sawtooth trailing edge and advanced control concepts to replace the function of the vertical tail. The next generation fighter needs a combination of all these things to fly under radar, while maintaining high agility characteristics. This will enable the vehicle to maintain high survivability and lethality over future battlefields¹⁷. This thesis will use the ICE101 configuration, which is suited for land-based operations, opposed to the ICE201 designed for operation off an aircraft carrier.¹⁷

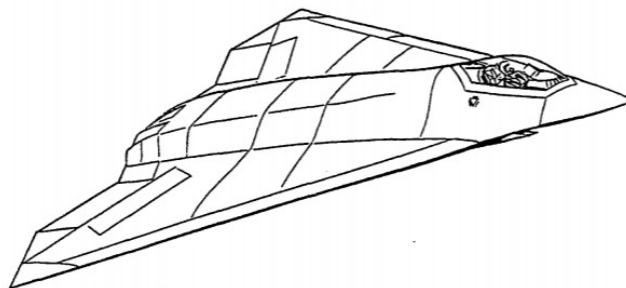


Figure 2.6: ICE-101 Configuration UAV¹⁸

Chapter 3

Computational Testing Methods

3.1 Traditional Methods

3.1.1 Introduction

Efforts in the conceptual design process for an aircraft are surrounded by the desire to optimize a certain aspect of its performance. For the analysis to be credible, the aircraft and environment need to be accurately represented in the design space. Not only is accuracy important, but the tool used needs to be efficient to allow a substantial number of design iterations. Throughout time, the methods of design have extensively changed to allow for higher fidelity predictions. From the Wright Brothers design based off of viable structural concepts from past experiences, to Prandtl developing the lifting line theory to implement a formal approach to solving wing aerodynamics. Since then numerous computational methods have been developed with a range of fidelities and uses. The overall level of available analysis tools far exceeds that of those from decades ago, and there will continue to be a need to shorten the time of the design process²⁸.

Today, the process of aircraft design involves empirical formulation, wind tunnel testing, full-scale experimentation, and a variation of computational analysis tools. Computational methods have greatly benefited the aircraft design process by improving the aerodynamics at conceptual and preliminary phases of design. Two types of commonly used computational aerodynamic analysis methods heavily used in contemporary design environments include potential flow-based approaches which rely primarily on surface or panel meshes, and volumetric (mostly Navier-Stokes) computational fluid dynamics (CFD) methods which rely on

volume meshes. Table 3.1 provides a general synopsis of the pros and cons of a range of aerodynamic analysis approaches.¹⁶

Table 3.1: Methods of Analysis¹⁶

	Empirical formulations	Potential flow methods	Computational Fluid Dynamics	Experimental methods
Complexity of input data/geometry	Low	Intermediate	Heavy	Heavy
Run time for single design	Low	Intermediate	Intermediate/Heavy	Heavy
Solution fidelity	Intermediate	Intermediate	Good	Good
Automation possibilities for optimization	Very high	high	Low	Very low
Range of physics	Limited	Limited	High	High
Cost of process	Very low	Low	High	Very high

3.1.2 Empirical Formulations

Empiricism is a very simple way of testing aircraft dynamics. Simple formulation (such as Holcomb’s area rule, linear aerodynamic models based on wing aspect ratio, skin friction from wetted area etc.), is still used at the initial stages of design and remains important to concept viability studies. In simple environments, these methods provide generally low to intermediate fidelity but may provide valuable guidance for the applicability of concepts.

3.1.3 Potential Flow Methods

Potential Flow Solvers are approaches which rely on the solution to a boundary value problem formulated by combining the continuity and momentum equations. By dropping the viscous terms, the resulting mathematical problem becomes conservative and is therefore amenable to solution using potential functions. Typically, the gradient of this potential provides the flow parameters of interest. Such methods do not involve the energy equation or dissipation

effects such as boundary layer momentum loss. Inviscid aerodynamics can be used to provide high fidelity solutions to subsonic flow around aircraft outside of the boundary layer at angles of attack up to the onset of stall.²² Generally the potential function can take on forms which are physically interpretable as sources or sinks, distributed circulation (usually referred to as vorticity), or a combination of the two. Classic analytic solutions using this approach include the inviscid flow over a cylinder or sphere, flow over an airfoil with the application of the Kutta condition, and Prandtl's lifting line approach. More modern implementations fit into the general genre of "panel methods." With the addition of mostly post processing viscous effect modeling, these methods can provide sufficiently high-fidelity aerodynamic analysis results to drive the outer mold line design. Since these methods only require surface meshes, they are typically far more computationally efficient than volumetric approaches rendering them applicable to optimization and design of experiments approaches during early to middle phase of design.²⁰ The main limitation potential solvers is the restriction placed on the range of applicable physics. For appropriate environments, these methods are highly effective.²¹

3.1.4 Computational Fluid Dynamics

Volumetric CFD became practical with the advent of digital computing devices and the series expansion-based formulations resulting in algebraic representations of the Navier-Stokes equations, first developed by McCormick and others in the 1960's and 1970's. Volumetric CFD can be broadly divided into solutions to the Euler equations with viscosity neglected and the full viscous Navier-Stokes formulation. CFD has evolved from its infancy to a reliable aerodynamic load prediction tool that greatly enables advancements of modern aircraft design. Numerical solutions to the Navier-Stokes equations for external flows is typically computationally expensive in cases requiring high fidelity. Nevertheless, with sufficient time and computational

resources, high fidelity solutions for subsonic, supersonic or hypersonic flow is achievable.^{4,21} CFD is even capable of assessing the interaction of propellers or rotors with the fuselage and other aircraft components with every increasing time and resources.²⁰

Despite the numerous benefits, contemporary numerical solution methods for the Navier-Stokes equations require significant learning curve, both volume and surface meshing, (which creates another layer of possible errors and stability issues) and extreme computation times depending on the complexity of the environment. Aside from limitations of usage and meshing, CFD has become a successful and widely applied tool for exploring a wide range of physics applications and is currently one of the primary tools in the aircraft design process.^{19,22}

3.1.5 Experimental Test Flights

Experimental flights typically provide the closest approximation to the intended flight of a vehicle under design. This mostly refers to a wind tunnel test, whether it is full-scale or scaled down, but can sometimes include the instrumented atmospheric flight of a test article. When conducting these tests, it is essential that the aircraft and in-flight conditions are properly scaled. If the flight conditions are not met or corrected for, then the measurements and or data analysis is susceptible to anomalies. This method of testing leads to an exceptionally high cost per design case when accounting for all the materials, construction, additional setup costs, and simply the cost of time. Since there is such a high price tag associated with it, this analysis is usually restricted to the later part of the design process.⁸

3.2 FlightStream®

3.2.1 Introduction

FlightStream® arose from the need for improvement in both computational time and efficiency in the earlier phases of aircraft aerodynamic design and optimization. FlightStream®

is a highly efficient subsonic, inviscid, surface-vorticity flow solver that does not require volumetric meshes.²⁰ Broadly, FlightStream® falls in the category of a panel based potential flow solver although FlightStream® is capable of resolving viscous effects associated with boundary layers and high lift scenarios. Many other computational tools have been developed to aid in this type analysis and research, but these methods have been hampered by non-intuitive implementation frameworks, incomplete physics modeling, and a lack of interface with modern complimentary engineering tools such as CAD and post processing. FlightStream® can conduct an analysis and produce a solution similar in fidelity for loads and moments to that of a Navier-Stokes solver applicable to early design analysis, but in a fraction of the time. FlightStream® is therefore an efficient and low-cost alternative solution to the aggregate aircraft aerodynamic design problem. Figure 3.1 illustrates where FlightStream® falls in relation to other solvers.

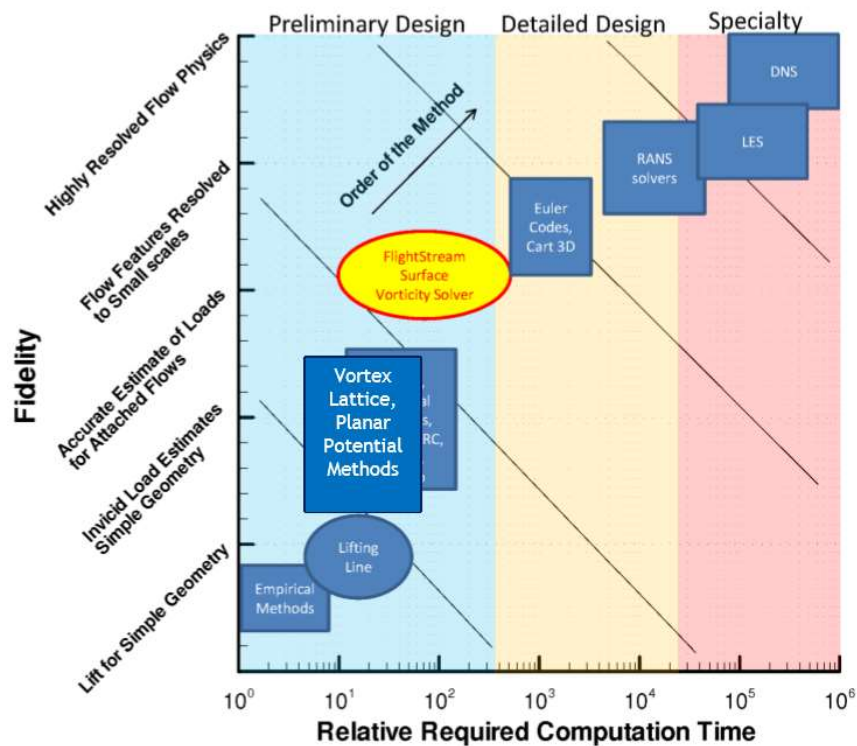


Figure 3.1: Method of Analysis Comparison¹⁶

3.2.2 Integration and Meshing

FlightStream® can fully integrate with numerous types of geometry imports from a variety of different aircraft configurations.¹⁹ These configurations included conventional and nonconventional geometries and blended bodies. For CAD import, FlightStream® typically requires .IGES file imports for CAD geometries and .STL file imports for mesh geometries. FlightStream® can handle all portions of the aircraft, such as wings, propellers, stabilizers, fins, nacelles, pylons, and fuselage sections. While handling these sections, it also has a tool to select and identify the individual parts of the aircraft, which is useful during the analysis.²⁰

Once the geometry is imported, FlightStream® offers a range of meshing options. Free surfaces are converted to trimmed surfaces internally. The anisotropic surface meshing tool allows for identifying and refining specific parts of the geometry. This allows for generating a computationally efficient, unstructured surface mesh. This benefit includes local refinement on curvatures as required, and isolated refinement on control surfaces. The meshing tool works automatically to generate these triangulated and quadrilateral meshes. During this process, the aircraft outer mold line fidelity as described by the CAD is maintained. After the automatic meshing, repair tools are available to address any remaining mesh anomalies. These tools include repairing holes, repairing missing patches, extruding curves, splitting patches, and editing curves. A workflow illustration is presented in Figure 3.2 to show the start, from CAD model input, to finish, with a simulation analysis. This entire integration can take a matter of seconds.²⁰

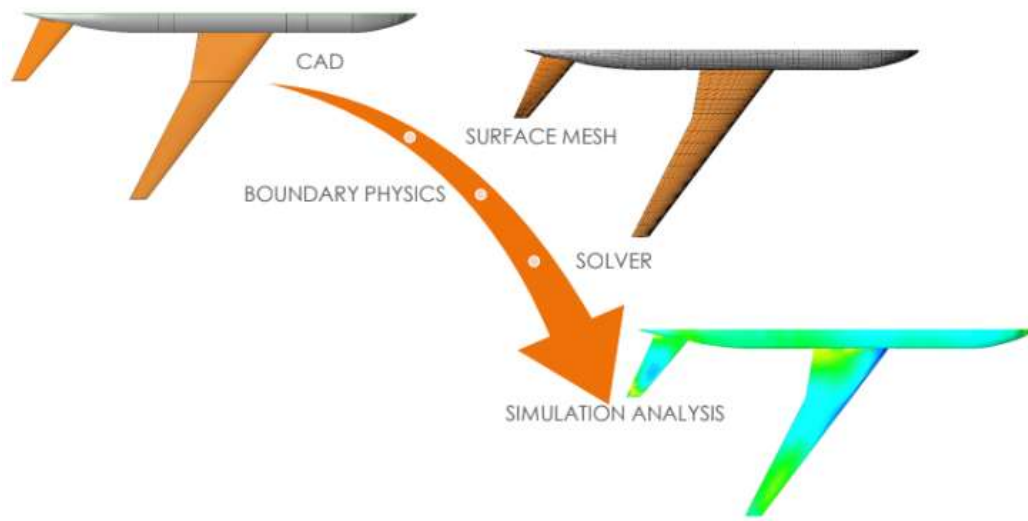


Figure 3.2: FlightStream Workflow¹⁶

3.2.3 Solutions

FlightStream® calculates loads using two optional methods. A direct application of the Kutta-Joukowski theorem can be fielded for fast solutions using relatively course meshes. Alternatively, a pressure based solution is available for more refined surface meshes. The pressure-based approach is required for more accurate treatment of boundary layers and for the implementation of the high lift capabilities available in the most recent editions of FlightStream®. The solution capabilities include that of handling flow field parameters, time resolved solutions, resolution of trailing vorticities, close-proximity solutions, and inviscid load calculations.¹⁹ FlightStream® has boundary physics properties that shed vorticity for generating aerodynamic loads. There are slip wall boundary conditions for all geometry surfaces applied during the potential portion of the solution with boundary layer analysis applied during post processing steps. FlightStream® has Prandtl-Glauret, Karmen-Tsein, and Latoine compressible and transonic flow modeling corrections available which are suitable for Mach numbers up to free stream value of Mach 0.85. FlightStream® rapidly computes stall and post-stall

aerodynamics from user-specific fluid properties and the solution for the surface vorticity distribution.²⁰

Inlet flow conditions, exhaust modeling and propeller interactions are all available. The gas turbine integration capabilities work through in conjunction of the NPSS tool. NPSS can be integrated into the aerodynamic solution by integrating engine performance and boundary conditions at the inlet and exhaust interfaces with FlightStream®.²⁰

3.2.4 Synopsis

FlightStream® is a vorticity-based aircraft centric computational flow solver that can calculate loads for a full complement of subsonic airplane configurations. In aerospace applications, there is a definitive trade between minimizing computation time and maintaining fidelity of the solution and the validity of the physics. FlightStream® strikes a cutting edge balance by producing solutions with sufficiently high fidelity to inform the design process in minutes or less per solution.²⁰

Chapter 4

Wind Tunnel Tests

4.1 Boeing KC-135 Stratotanker Case Study

4.1.1 Introduction

The case study used was conducted to investigate the possibility of adding winglets to the KC-135 for performance improving reasons. This test used the basic configuration for a KC-135, but along with the trail of winglet designs. This research only covers the baseline configuration.²⁶

4.1.2 Wind Tunnel Setup

A 0.035 scale model of the KC-135 was made for this testing at the NASA Langley Research Center. Its data was collected at the Langley 8-foot transonic wind tunnel. The model included nacelles, a vertical stabilizer and a horizontal stabilizer. It was sting mounted and contained internal strain gauges for measuring data.²⁶ These tests were set to replicate flight conditions at a 30,000 feet cruise and a freestream velocity of 292 ft/sec. A three-view schematic of the aircraft is shown in Figure 4.1. The aircraft characteristics are given in Table 4.1, along with the scaled down data.

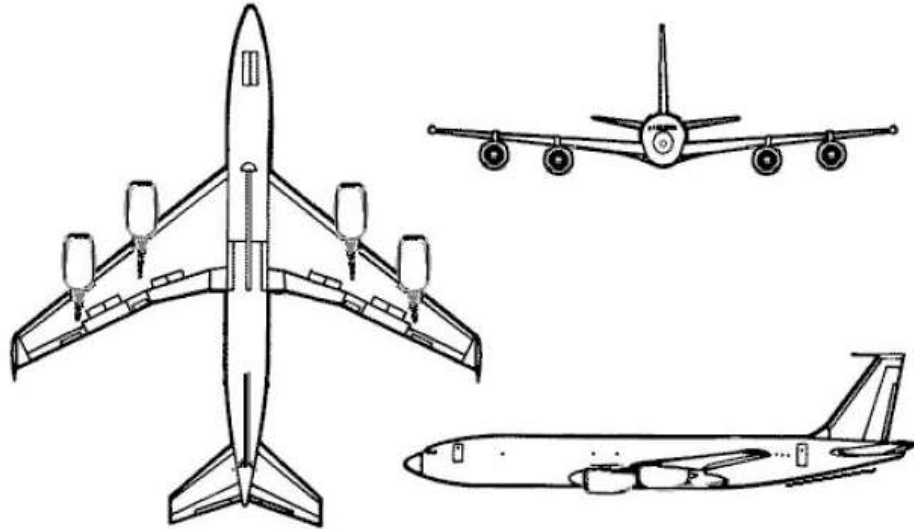


Figure 4.1: Boeing KC-135 3-View Schematic²⁶

Table 4.1: Boeing KC-135 Characteristics

	Full-Size Model	0.035 Scale Model
Wing Reference Area	81.5	2.91 ft ²
Wing Reference Chord	19.32ft	8.28 in
Wing Reference Span		54.60 in
Length	136ft 3 in (41.53m)	4.76875 ft (1.45355m)
Wingspan	130 ft 10 in (39.88m)	4.5791 ft (1.3958m)
Height	41 ft 8 in (12.70m)	1.458 ft(0.4445m)
Wing Area	2433 ft ² (226m ²)	85.155 ft ² (7.91m ²)

4.1.3 Results

The results from the wind tunnel tests are shown in Figure 4.2 with and without the winglets added to see the difference in lift per angle of attack. The winglets results are not of interest in this study, so the solid line result is the focus for this work.²⁶

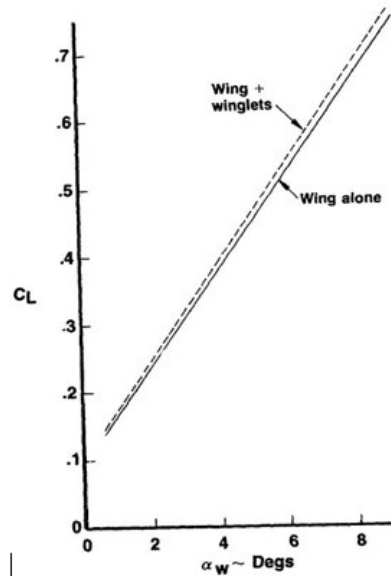


Figure 4.2: KC-135 Coefficient of Lift vs. AOA²⁶

4.2 ICE-101 Configuration UAV Case Study

4.2.1 Introduction

To realize the full potential of future UAVs in-flight refueling capabilities will be required. This would benefit range and rapid deployment options and allows long distance strikes. A baseline UAV configuration was sought to develop this aircraft. This need led to the Innovative control effectors program to develop this realistic aircraft.²⁴

4.2.2 Wind Tunnel Setup

The ICE-101 Configuration UAV is a Lockheed delta wing tailless aircraft. It is a single engine design and consists of two narrow inlets on the lower surface.²³ It was developed at the Air Force Research Labs. During its formation it was subject to extensive wind tunnel testing to

be further cleared for public release. The Figure 4.3 below is an example of the configuration used in this research and Figure 4.4 shows the control surface allocation²³.

The ICE-101 Configuration UAV were tested individually. The inlets on the lower surface of the aircraft were blocked for the tests described. There were two models available for testing, both were 0.077 scale models of the actual aircraft. Table 4.2 identifies the UAV aircraft parameters at both full scale and the scale it was tested in.²⁴ While scaled to the same size, the aircraft models were created by different companies, years apart, so there were slight differences. Model B was made later and has slight bumps to accommodate control surfaces.²³

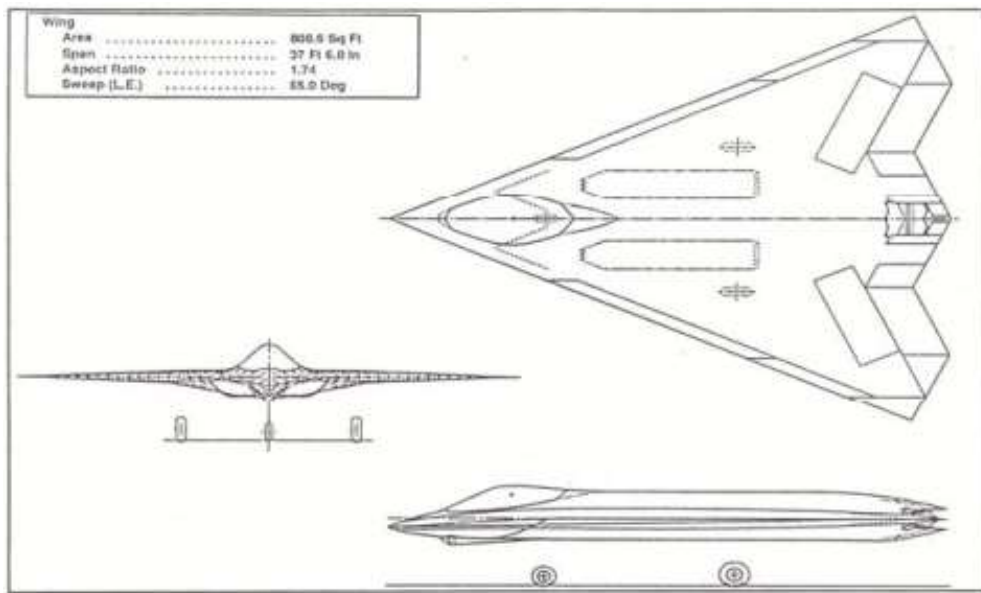


Figure 4.3: ICE-101 Configuration UAV 3-View Schematic²³

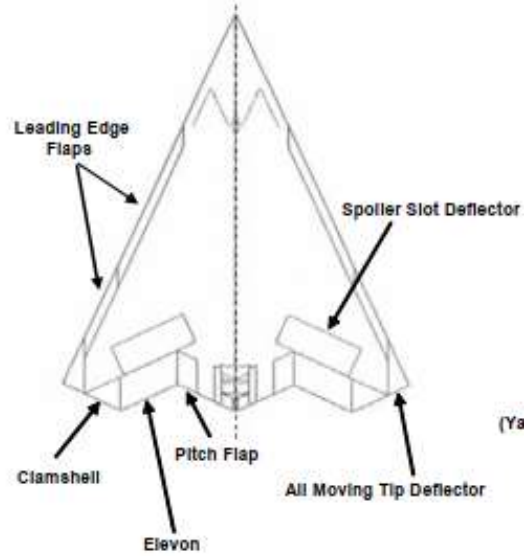


Figure 4.4: ICE-101 Configuration UAV Control Surfaces²³

Table 4.2: ICE-101 Configuration UAV Characteristics

Configuration Geometry Scale	Full	0.077
LE Sweep (deg)	65	65
TE Sweep (deg)	25	25
Body Length (in)	517.49	39.81
Wingspan (in)	450	34.62
Reference Wing Area (sq ft)	808.58	62.2
Reference Wing Aspect Ratio	1.74	1.74
Reference Wing MAC (in)	160.68	12.36

4.2.3 Results

Each model, A and B, were tested individually in isolation for its coefficient of lift per angle of attack. There were multiple configurations and facilities used in this test. From the

multiple designs, time of creation, and material used there were also slight differences in the wind tunnel data as shown in Figure 4.5 below.

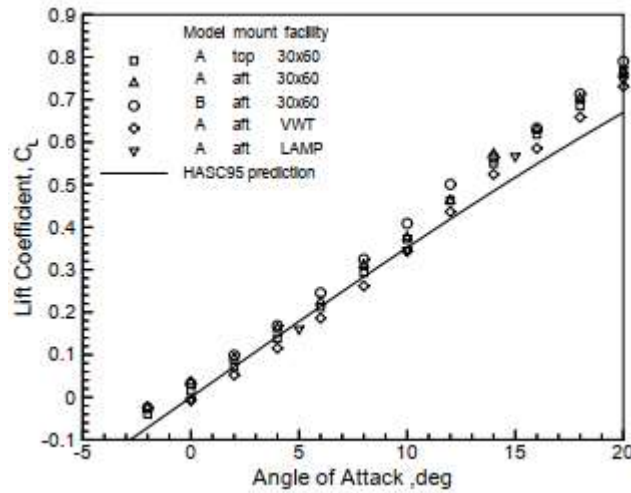


Figure 4.5: Individual UAV Coefficient of Lift vs. AOA²³

The results for each model and each configuration shown are very similar and seen as acceptable for the testing project. The differences in model material, wind tunnel configuration, and “bumps” are acknowledged as the reason for the very minor differences in results. In the study used, the researchers used the wind tunnel tests to compare to a vortex lattice HASC95 prediction method, which is represented with the line in the results. This is not of importance in this research.²³

4.3 UAV Formation Flight Case Study

4.3.1 Wind Tunnel Set-Up

The same wind tunnel tests used to test the UAV individually was used in the formation flight tests. All runs were conducted at a tunnel dynamic pressure of 5 psf or a corresponding speed of approximately 65ft/sec. Both models were then configured with six internal component strain gauge balances to make measurements. Model A was the lead aircraft and model B was used as the trail aircraft during the maneuver. The setup of rods used to hold each model in place

was determined to minimize rig interference effects on the trail model. An image of the setup is illustrated below in Figure 4.6. Figure 4.7 illustrates how the trail aircraft will encounter lateral spacing through this testing.²³



Figure 4.6: Wind Tunnel Formation Flight Setup²³

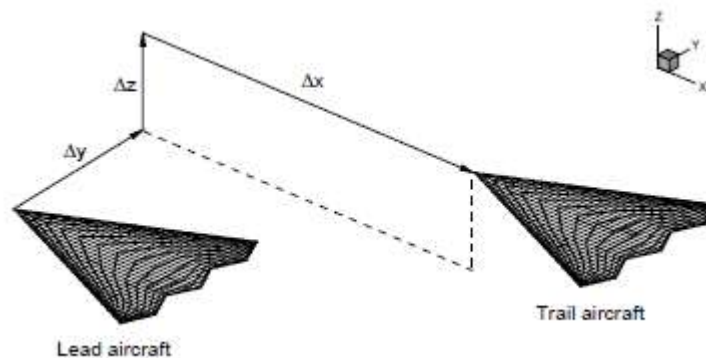


Figure 4.7: Vertical, Lateral, and Longitudinal Spacing²³

4.3.2 Results

The formation flight results primarily focus on the lateral spacing of the aircrafts. There is no vertical spacing in these tests. Each aircraft is on the same relative plane to the oncoming wind. The longitudinal spacing is set at $x/b = 2$ for the duration of this test. The lead aircraft is set to an angle of attack of 8 and the trail aircraft is shown to have results at both 0 and 8. The results in this thesis primarily focused on that of 0 angle of attack. The effect of this spacing on

the wake induced lift is shown in Figure 4.8 below.²⁷ Since the results with the angle of attack of zero is of interest, Figure 4.9 is produced below to emphasize those results. The solid line represents a vortex lattice method that the previous testing compared its wind tunnel data to and is not of interest in this thesis.

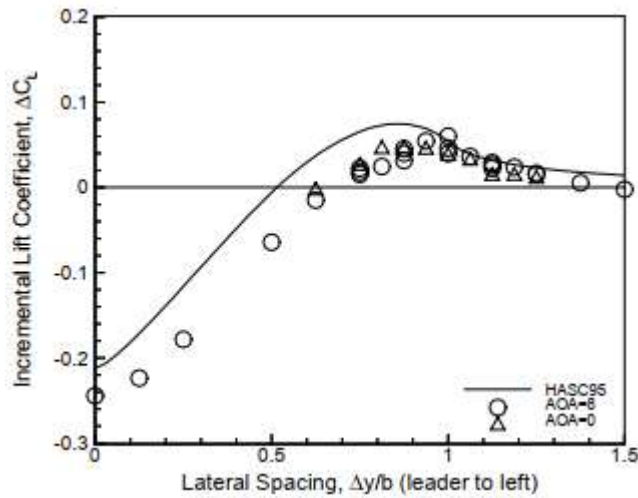


Figure 4.8: Formation Flight Coefficient of Lift vs. Lateral Spacing²⁷

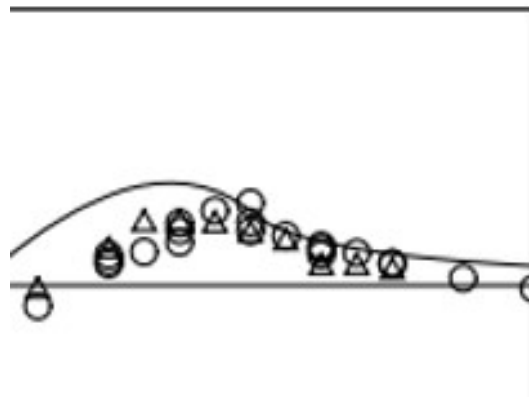


Figure 4.9: Trail Aircraft AOA 0 Results²⁷

The results of this formation flight show that as the trail aircraft moves outboard of the lead aircraft lift loss reduces and up wash occurs and reduces once passing the lead aircraft's wing tip, meaning $y/b > 1$.²³

4.4 Aerial Refueling Case Study

4.4.1 Introduction

The purpose of aerial refueling is to also increase the range of the receiving aircraft. This creates the ability to increase loiter time for surveillance aircraft, which is what many UAVs are used for in the USAF. These wind tunnel tests were a part of a larger scheme to demonstrate autonomous refueling efforts of a UCAV. UCAVs are UAVs capable of carrying bomb loads in excess of 1000 lbs. These types of aircraft are generally lighter with smaller moments of inertia, thus aggravating the effects of turbulence encountered behind a tanker.²⁵

The wind tunnel data used for comparison is from a test of the ICE-101 Configuration UAV flying behind a KC-135 tanker. These results show the wake interference effects on the UAV from different lateral and vertical positions. There are longitudinal changes as well but not much of a significant wake interference from the positions studied. The tail and wing of the tanker is shown to have the strongest effect on the receiver's aerodynamics.²⁵

4.4.2 Wind Tunnel Set-Up

These wind tunnel tests were run to assess the stability and control characteristics of the UAV in the tanker wake. This will help develop a database for simulation and control law development. The tests were held at the Langley Full Scale Wind Tunnel run by Old Dominion University²⁵. Both the tanker and receiver were tested with a 0.077 scale model. Table 4.3 illustrates the scaled down parameters of the KC-135, since the previous data was different. The tanker held four electric fans to simulate engine thrust. The tanker was attached at the top of its fuselage to the flow survey carriage to minimize rig interference, and the receiver was mounted from the bottom to a post on the tunnel floor. Both aircraft were equipped with internal six

component strain gauge balances to help record data. A reference of the two full-scaled aircraft side by side is shown below in figure 4.9.²⁵

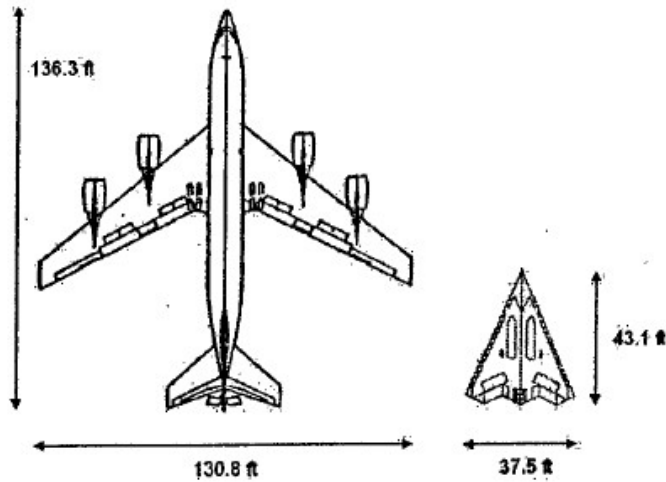


Figure 4.10: Aircraft Models Comparison²⁵

Table 4.3: Boeing KC-135 0.077 Characteristics

	Full-Size Model	0.077
Wing Reference Area	81.5	6.275ft
Wing Reference Chord	19.32ft	1.48ft
Wing Reference Span		109.2in
Length	136ft 3 in (41.53m)	10.49ft
Wingspan	130 ft 10 in (39.88m)	10.07ft
Height	41 ft 8 in (12.70m)	3.21ft
Wing Area	2433 ft ² (226m ²)	187.341ft

When performing the testing, the tanker and receiver were set at differing angle of attacks. The tanker was set at an angle of attack of 2 degrees. The receiver was set at an angle of attack of 4 degrees. The flight conditions correlate with 29,000 ft in altitude and a dynamic pressure of 5 psf, corresponding to a speed of 65 ft/sec.²⁵

4.4.3 Results

The results focus on the effect of lift on the receiver against lateral spacing from behind the tanker. Lift is measured at two different longitudinal spacings, that of $x/b = 0.85$ and $x/b = 3$, which represents 20 feet and 300 feet at a full scale behind the tanker. Since there is not much difference in results due to longitudinal spacing, the results from this thesis will focus on the 20 foot scale. Vertical spacing is measured from c.g. to c.g. and a vertical spacing of 0 is used in this experiment.²⁵

Lateral spacing is the main emphasis of research here. This refers to the relative lateral position between the two aircraft on the X-Axis. These values are non-dimensionalized by the span of the tanker. A value of 0 refers to when the two aircraft are directly aligned with their centers. A value of 0.5 refers to when the nose tip of the receiver is perfectly lined up with the tip of the tankers left wing, then the wing tips are aligned at a value of 0.64. The lateral positioning results is shown below. The solid line is data with a horizontal tail incidence of -8 and the dotted line refers to a horizontal tail incidence of 0 for the tanker. This research will focus on the case with the horizontal tail incidence set to zero. In this aerial refueling environment, the receiver shows a large lift loss when immediately behind the tanker, until the receiver approaches the tanker wing tip.²⁵

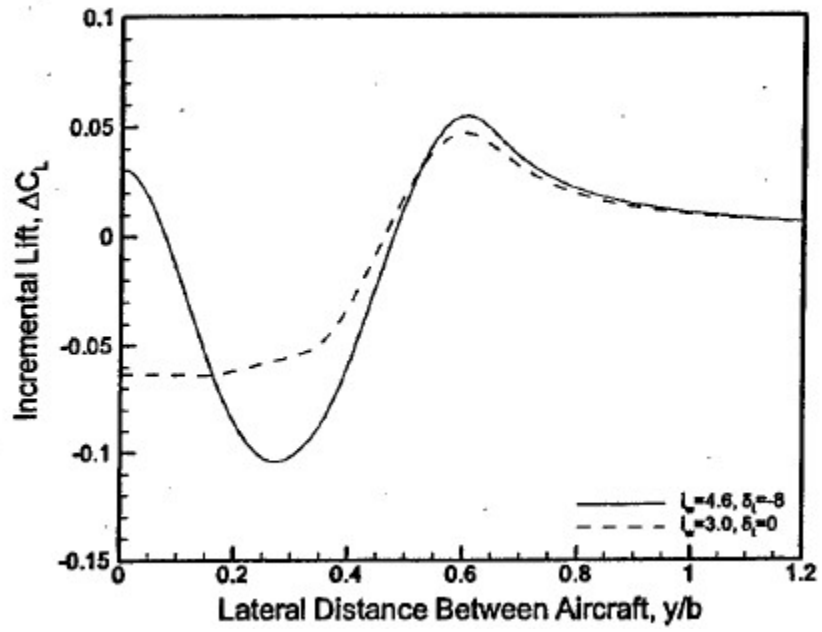


Figure 4.11: Aerial Refueling Wind Tunnel Results²⁵

Chapter 5

FlightStream® Analysis

5.1 NASA Vehicle Sketch Pad

5.1.1 Introduction

All models used in the research were developed in NASA's Open Vehicle Sketch Pad (OpenVSP) software. In the process of designing and analysis of aircraft in computational space, there has been a long-standing requirement for efficient and accurate geometric representations of the vehicle early in the design cycle. Vehicle Sketch Pad (VSP) was developed as an intuitive, open source, and efficient method to fill a void for conceptual and preliminary design studies. VSP allows the engineer to very efficiently create an adequate outer mold line representation of the aircraft geometry for conceptual level aerodynamic analysis.¹⁵

VSP is a geometry-modeling program specifically designed for use in the conceptual stage. At this stage, the methods of design should be fluid and allow for ease of change in large geometries to test a broad design space. This task is not easily achieved in a CAD program. VSP works directly with aircraft geometric parameters such as wingspan, airfoil definition, span, and fuselage diameter and therefore fits the mold geometry representation well. With scripting, the geometry engine inside VSP can be included in an optimization pipeline along with tools such as FlightStream® to predict aerodynamic loads in a design study.¹⁹

5.1.2 Integration and Meshing

VSP is highly integrated with FlightStream®. Mesh files can be directly imported into FlightStream® and are mostly, solver ready. There are cases with more complex geometries that require multiple parts to be combined in VSP, such as a fuselage, wings, and nacelles. In this

scenario VSP has a CompGeom tool to combine these parts into a single mesh for a seamless transition into FlightStream®. CompGeom is an efficient one-click tool mesh refinement tool that generates high-quality anisotropic quads and unstructured isotropic triangular meshes. This keeps the mesh sizes small in terms of face count to allow the solver to run fast and accurately. The geometry must be exported out of VSP as a .STL file for an easy FlightStream® geometry import. Sometimes a small amount of repair and adjustments will need to be made, but that can generally be accomplished in FlightStream®.¹⁹

Mesh generation is classified in two main groups, the structured and unstructured mesh. Structured methods are algebraic generators based off of mapped transformations between a natural and physical domain. Unstructured methods use geometry as reference to generate the mesh. Triangular mesh tools automatically discretize complex geometries, but often perform poorly in linear displacement version. Quadrilateral structured methods create smooth meshes and provide good control of the aspect ratio of the elements but depends on geometric decomposition techniques to mesh complex configurations with fully automated schemes. Unstructured mesh generation methods take advantage of the automation of their algorithms and the good performance of the quadrilateral elements. It creates these elements by combining triangles generated²⁹. FlightStream® allows meshing OpenVSP CAD models in seconds. An unstructured quadrilateral surface mesh is generated.

5.1.3 Boeing KC-135 Stratotanker Model Geometry

The Boeing KC-135 model for the computational analysis was created in VSP. To develop the model a combination of data on the actual aircraft was needed. Figure 4.1 represents a three-view model of the KC-135, which was used to help develop the shape of the aircraft by following its guidelines for the fuselage, wings, vertical stabilizer, horizontal stabilizer, pylons,

and nacelles. Table 4.1 was used in conjunction with the three-view image to match the exact characteristics of the KC-135 tanker. A clean configuration is used in this analysis replicating that of the wind tunnel configuration. A clean configuration is that in which all flight controls are neutral to create minimum drag. This means flaps and gear are retracted. The KC-135 Tanker has four airfoil sections, as shown in Figure 5.1 where they are located. The exact airfoil shape is illustrated in Figure 5.2 and .DAT files of each airfoil shape was integrated into the proper location with VSP's available tool for implementation. A full representation of the model created in VSP is also shown below with a left, top, front, and ISO view of the aircraft in Figures 5.3 – 5.6. For computational analysis reasons a model of the KC-135 was also created without the pylons and nacelles as shown in Figure 5.7 – 5.10. Both versions of the aircraft need to go through the CompGeom tool to fill the gaps in the original mesh geometry shown in Figure 5.11 and 5.12. A half model was generated and imported into FlightStream® to reduce the number of mesh volumes and reduces testing time in general. Once in FlightStream, a symmetry tool is used to replicate a full model to resemble the wind tunnel tests.

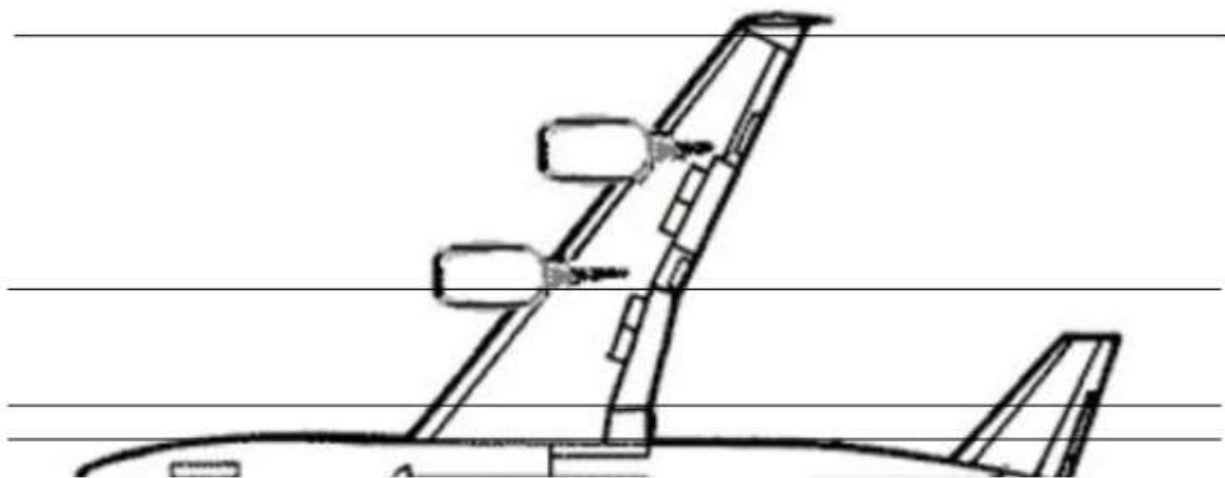


Figure 5.1: Boeing KC-135 Airfoil Location



Figure 5.2: Boeing KC-135 Airfoils

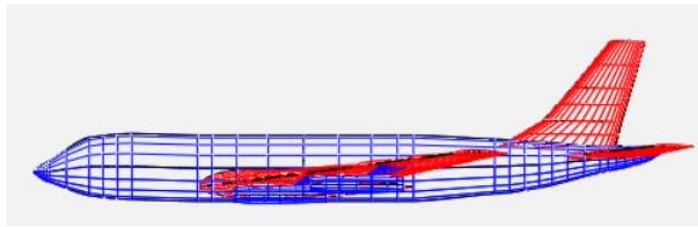


Figure 5.3: Boeing KC-135 Left View

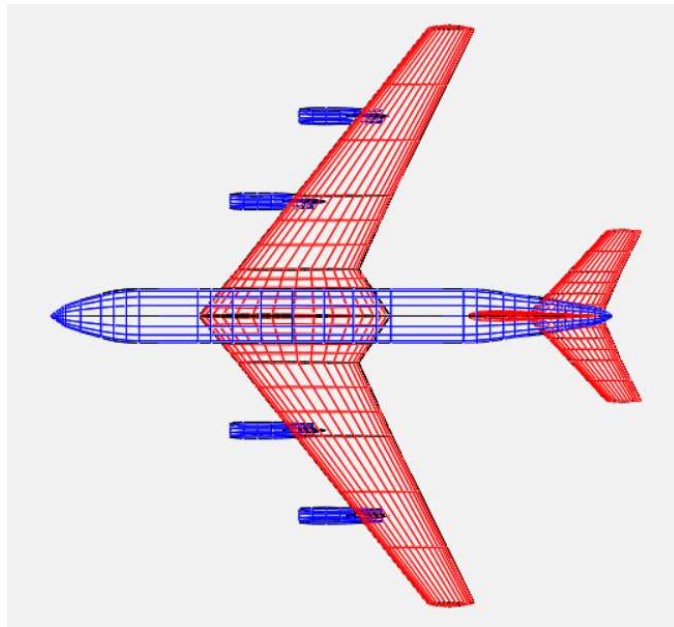


Figure 5.4: Boeing KC-135 Top View

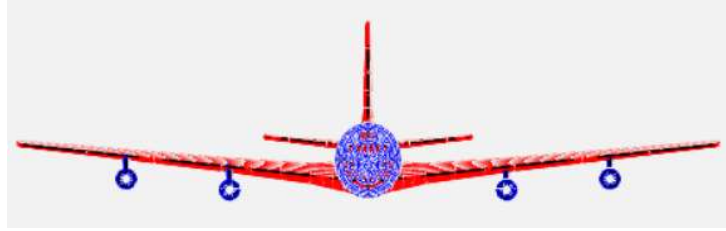


Figure 5.5: Boeing KC-135 Front View

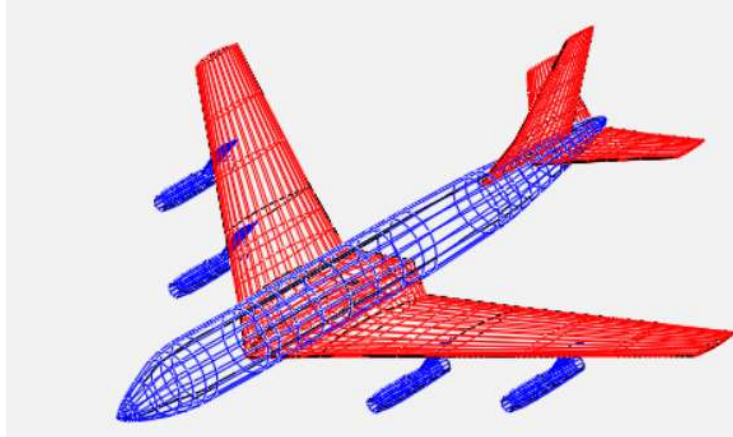


Figure 5.6: Boeing KC-135 Left ISO View

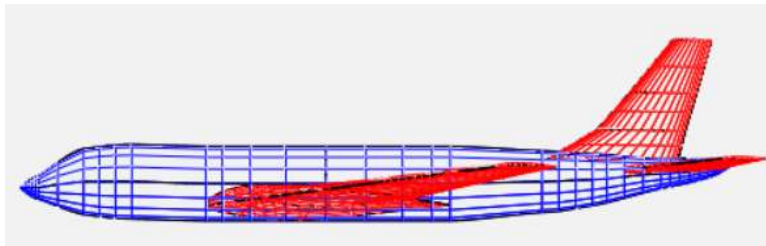


Figure 5.7: Boeing KC-135 Left View without Inlets

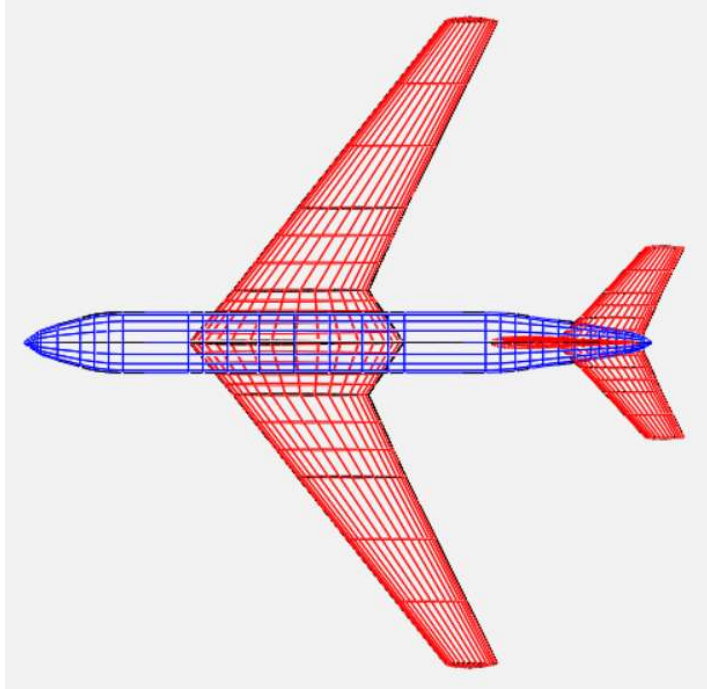


Figure 5.8: Boeing KC-135 Top View without Inlets

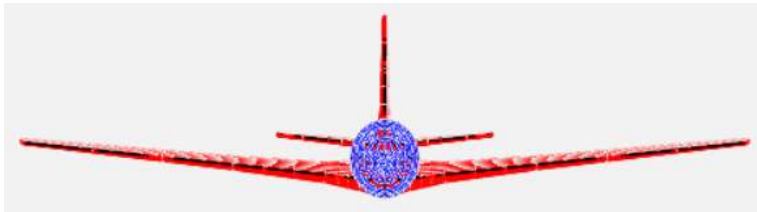


Figure 5.9: Boeing KC-135 Front View without Inlets

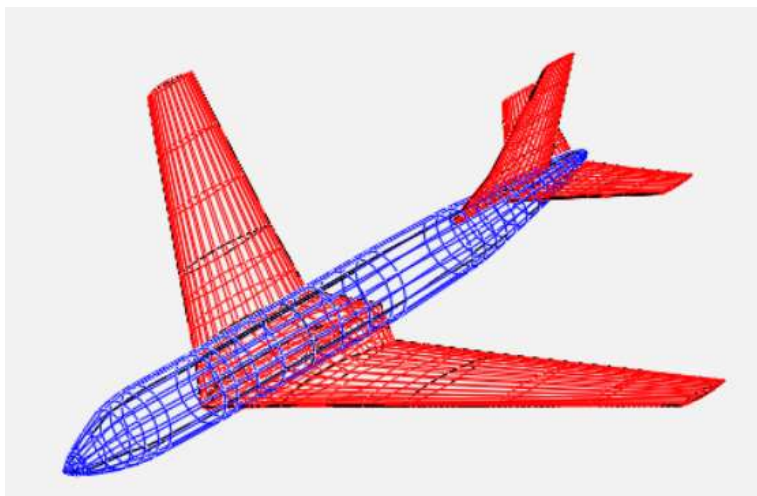


Figure 5.10: Boeing KC-135 Left ISO View without Inlets

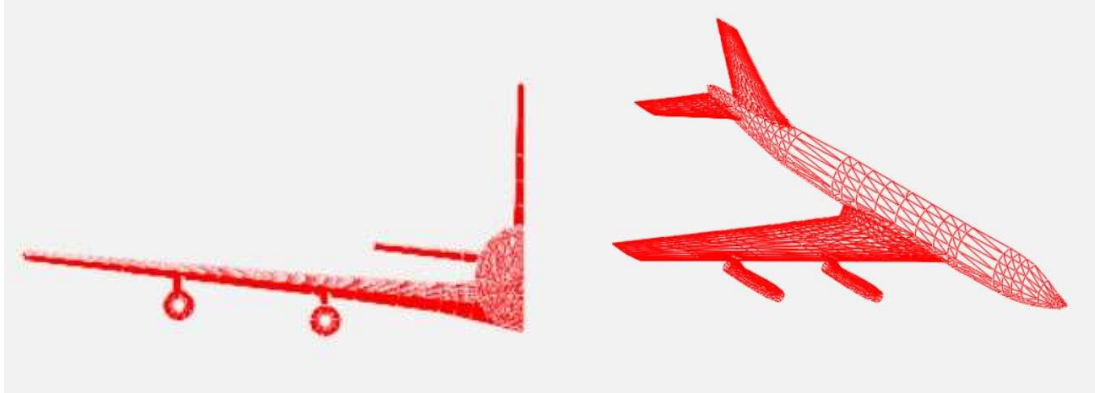


Figure 5.11: Boeing KC-135 CompGeom View

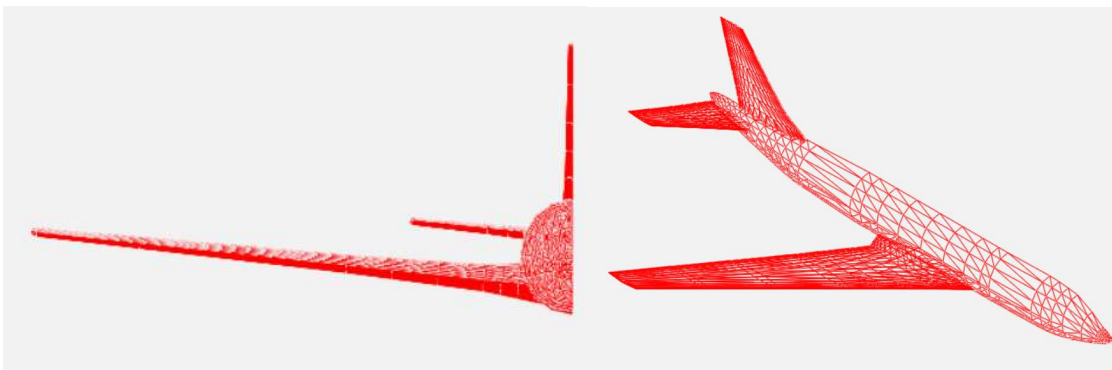


Figure 5.12: Boeing KC-135 CompGeom View without Inlets

5.1.4 ICE-101 Configuration UAV Model Geometry

The ICE-101 Configuration UAV model was also created in VSP. Aircraft characteristics were compiled with the use of the three-view model to create this geometry. Table 4.2 shows these desired characteristics to represent the actual aircraft, and Figure 4.3 was used in conjunction with those characteristics to develop the VSP model. A clean configuration is used in this analysis replicating that of the wind tunnel configuration. A clean configuration is that in which all flight controls are neutral to create minimum drag. This means flaps and gear are retracted. Differing from the KC-135, this UAV consists of only one airfoil, which is a NACA 0012³⁰. After the airfoil coordinates were generated, the model went through VSP's CompGeom

integration tool for mesh refinement and exported as a .STL file for further analysis. Figure 5.13 – 5.16 illustrate the UAV from multiple views. Figure 5.17 shows reference to the model after the CompGeom integration tool. A half model was generated and imported into FlightStream®. A half model is used to reduce the number of mesh volumes and reduces testing time in general.

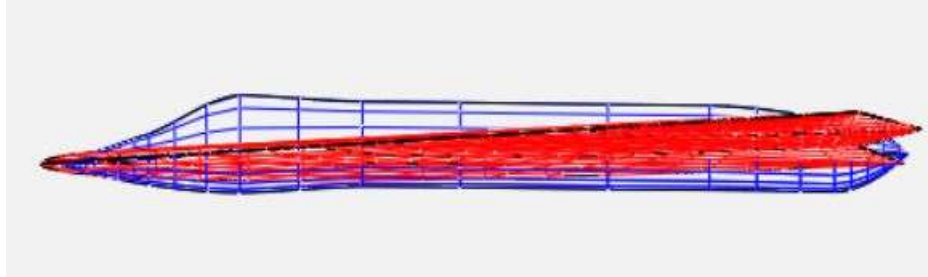


Figure 5.13: ICE-101 Configuration UAV Left View

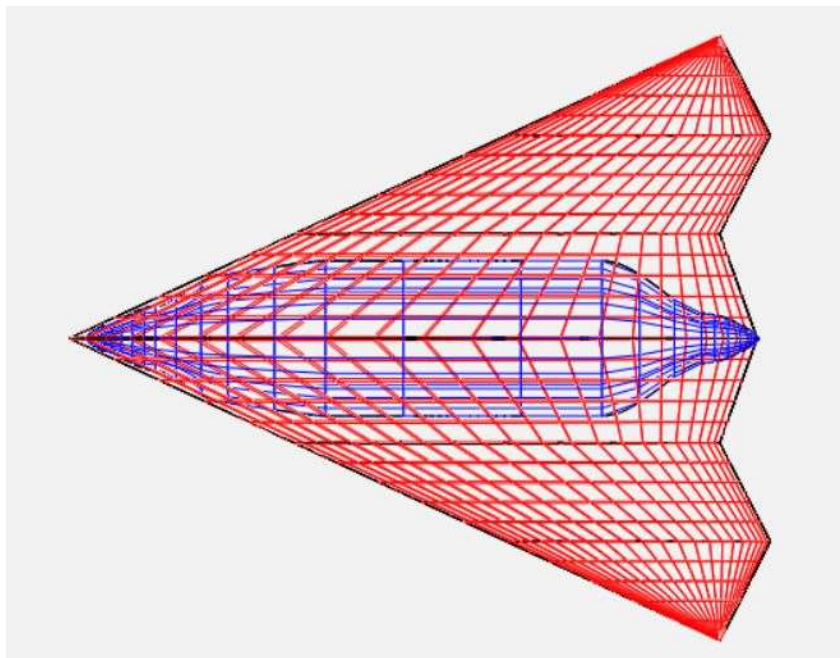


Figure 5.14: ICE-101 Configuration UAV Top View

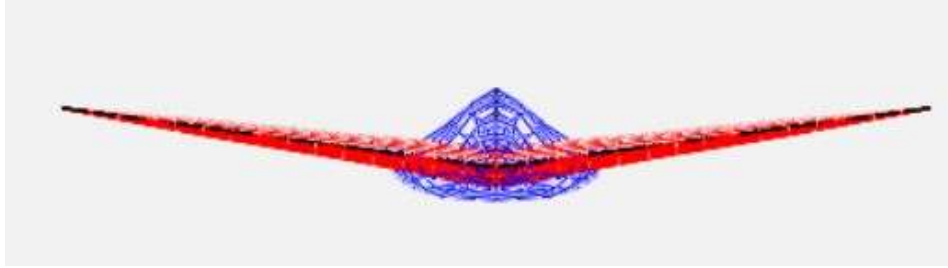


Figure 5.15: ICE-101 Configuration UAV Front View

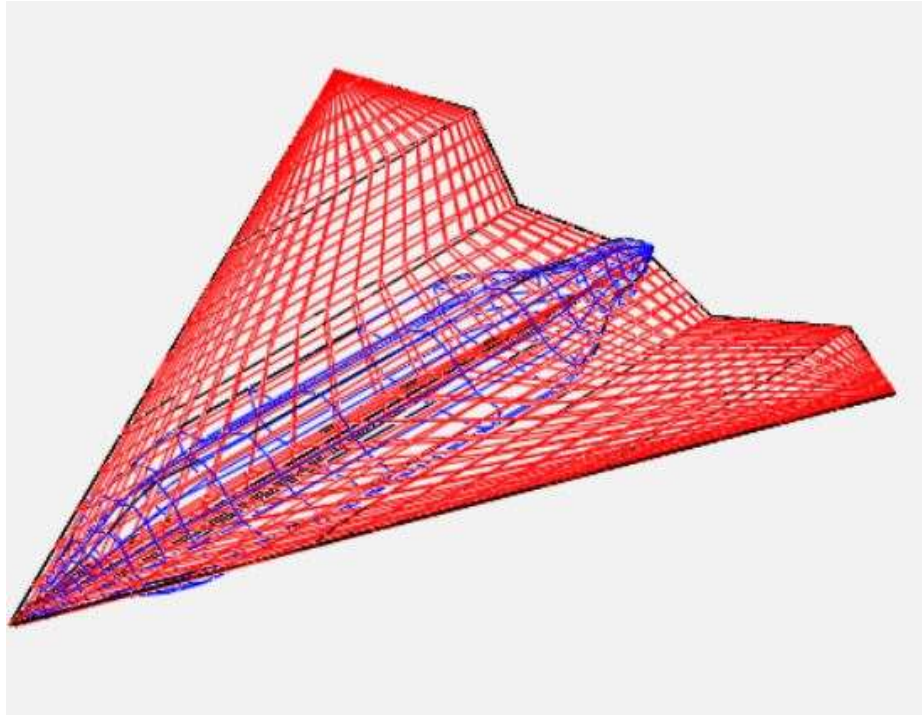


Figure 5.16: ICE-101 Configuration UAV Left ISO View

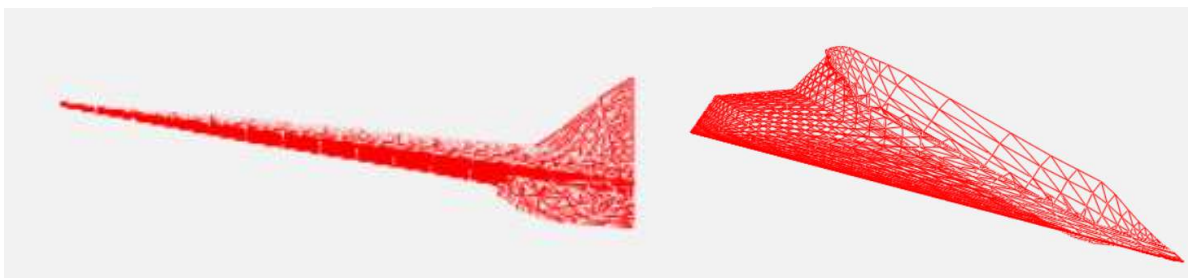


Figure 5.17: ICE-101 Configuration UAV CompGeom View

5.2 FlightStream® Computational Analysis

5.2.1 Introduction

This research compares FlightStream® predictions on a receiver in these close-proximity maneuvers, with that of previous wind tunnel data. This study initiates with individual analysis of each aircraft alone, followed by the complex scenarios. The data focus on the coefficient of lift versus certain angle of attacks for each aircraft. Those results were gathered in an effort to show the coefficient of lift of the trail aircraft versus the lateral spacing behind the tanker. These results are compared to the wind tunnel information described in Chapter 3.

5.2.2 ICE-101 Configuration UAV Validation Study

There were two separate UAV models made for the research conducted shown in Figure 4.6. Model A and B were created at different times and of different material. The model and mounting location for the results provided are shown in the key from Figure 4.5. The line represents a vortex lattice method. Models A and B are 0.077 scale of the actual aircraft. All of the scaling characteristics were described in chapter 4. The Wing Reference Area of 62.2 square feet and Wing Reference MAC of 12.68 inches (1.03 feet) are used in the desired FlightStream® solver locations to produce the correct results. All runs were conducted at a wind tunnel dynamic pressure of 5 psf and 65 ft/sec.

After inputting the correct aircraft conditions and wind tunnel data, FlightStream® can be used to produce the results compared with the wind tunnel data. The wind tunnel data is illustrated with a dot and FlightStream® is illustrated with a solid blue line. FlightStream® can accurately predict the aircraft coefficient of lift at the given angle of attacks in reference to the wind tunnel results it is compared too. Figure 5.18 illustrates the results produced in FlightStream®.

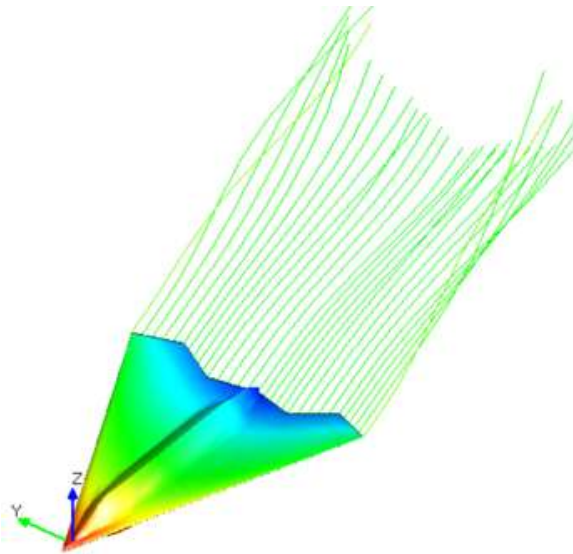
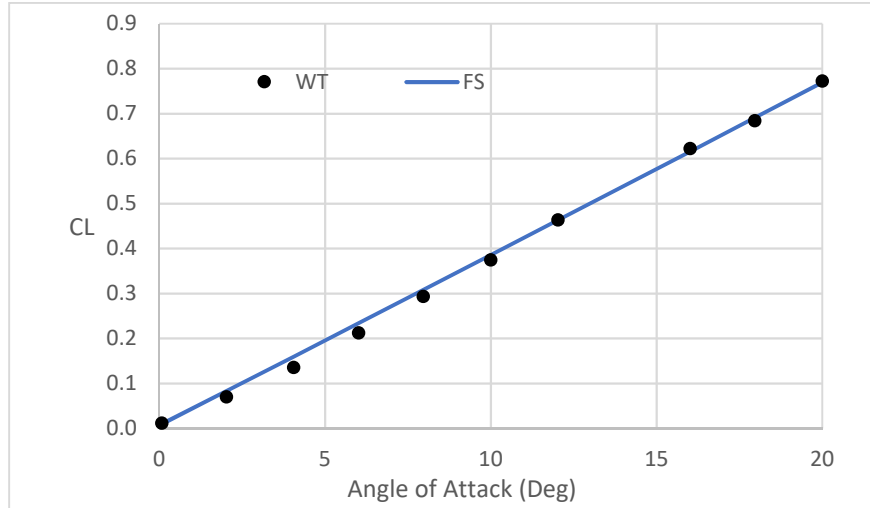


Figure 5.18: ICE-101 Configuration UAV FlightStream® Analysis

5.2.3 UAV Formation Flight Validation Study

After validating the UAV in isolation, a formation flight analysis was conducted with the same aircraft scaling and wind tunnel data used above. Figure 5.19 shows the effect of lateral spacing on wake induced lift of the trailing UAV. The results are for a longitudinal spacing (x/b) of 2 spans and vertical spacing of 0. An illustration of spacing with the lead and trailing aircraft is illustrated in Figure 4.7. At a lateral spacing of 0.5 the trailing aircraft's nose is aligned with the

lead aircrafts wing tip. At a lateral spacing of 1, the trailing aircrafts left wing tip is aligned with the lead aircrafts right wing tip. This spacing scale was used to generate the rest of the positions. My research focused on the spacing of the trail aircraft at an angle of attack of 0, illustrated by a triangle in the figure below. That portion is zoomed in and reproduced in the figure on the right of figure 5. This is representative of a lateral spacing of 0.5 to 1.25.

After inputting the aircraft used in isolation into the correct formation environment and including the same wind tunnel conditions used previously, FlightStream® produces the following results. The graph below is the wind tunnel data, illustrated with a dot, compared to the FlightStream® results, illustrated with a solid blue line, for the spacing mentioned above.

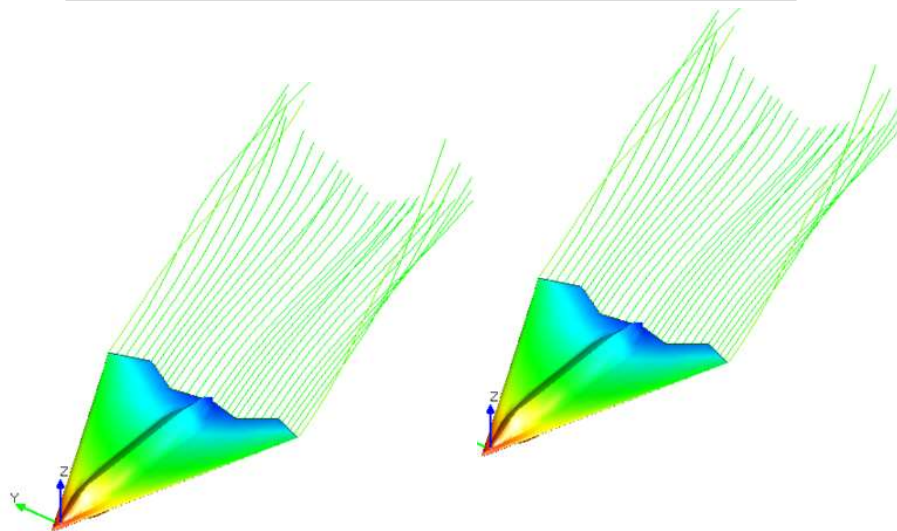
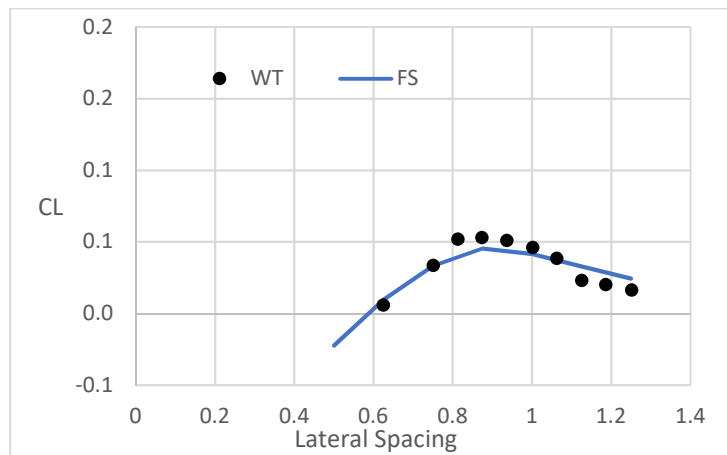


Figure 5.19: Formation Flight FlightStream Analysis

5.2.4 Boeing KC-135 Stratotanker Validation Study

The KC-135 is a tanker commonly used in the military for aerial refueling purpose. The figure above was research used to show the differences or benefits in adding winglets. My research focuses on the aircraft configuration without winglets. The model of the aircraft used in the research that generated the wind tunnel data is shown below. It was set to a 0.035 scale at Mach 0.3 and normal cruise conditions at 30,000 feet. Wing reference area 2.91 ft and wing reference chord 8.28in (4.55 ft) are used in the FlightStream® solver settings to generate the results.

After properly scaling the aircraft and inputting the correct wind tunnel conditions, FlightStream® was able to generate the results shown in Figure 5.20. A geometry without nacelles/inlets was used in this comparison. The wind tunnel, Inlets, and non-inlet configurations are all shown in Figure 5.20. (Differences with the inlets being lower could have to do with the engine integration tool, NPSS, in FlightStream® not being implemented, or the fact that enough iterations could not be run on my old computer to complete the analysis at higher angle of attacks.) The results without inlets are of sufficient fidelity for conceptual level design analysis.

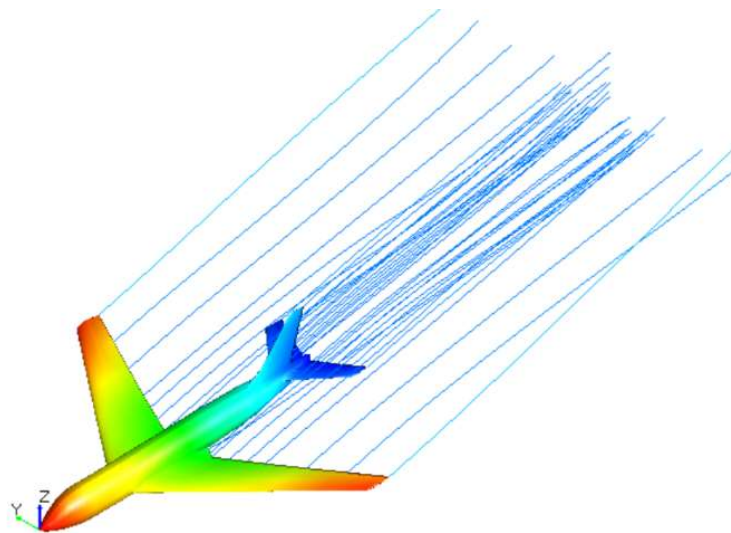
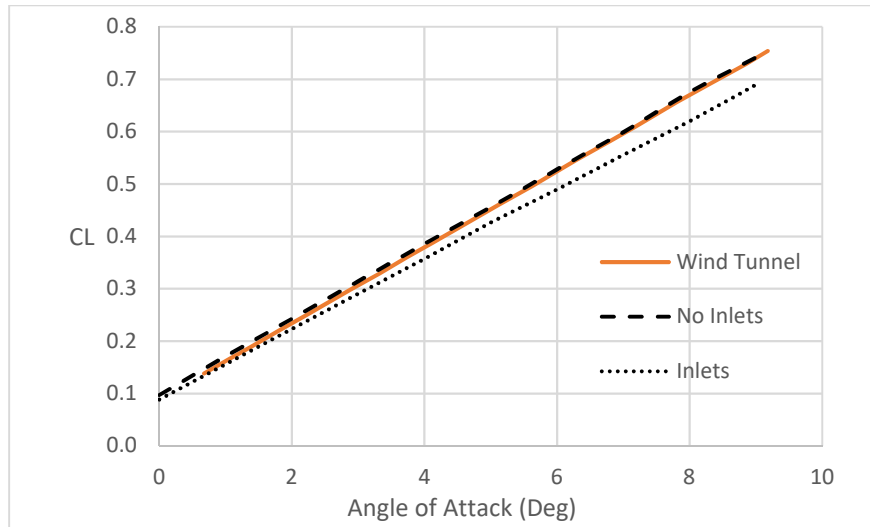


Figure 5.20: Boeing KC-135 0.035 Scale FlightStream® Analysis

5.2.5 Aerial Refueling Validation Study

The KC-135 was used in conjunction with the ICE-101 Configuration UAV to replicate an aerial refueling environment. The KC-135 for this experiment was a 0.077 scale model as well as the UAV. Previous work included a KC-135 at 0.035 scale, so below, in Figure 5.22, is also a FlightStream® analysis with the KC-135 scaled to 0.077 to be used in the aerial refueling analysis.

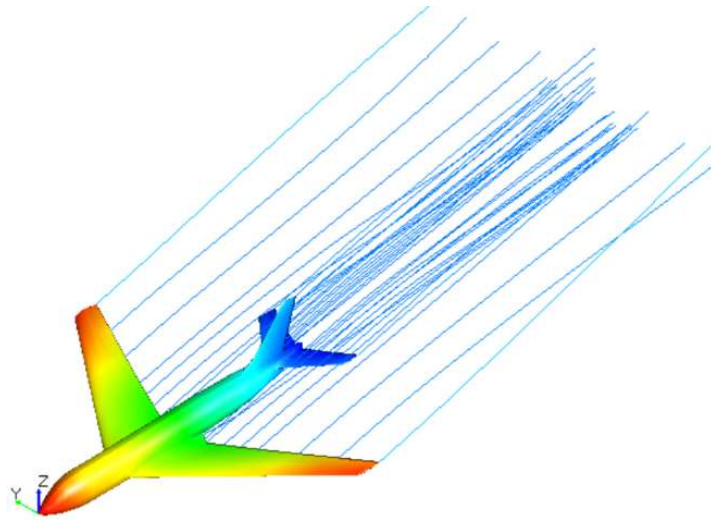
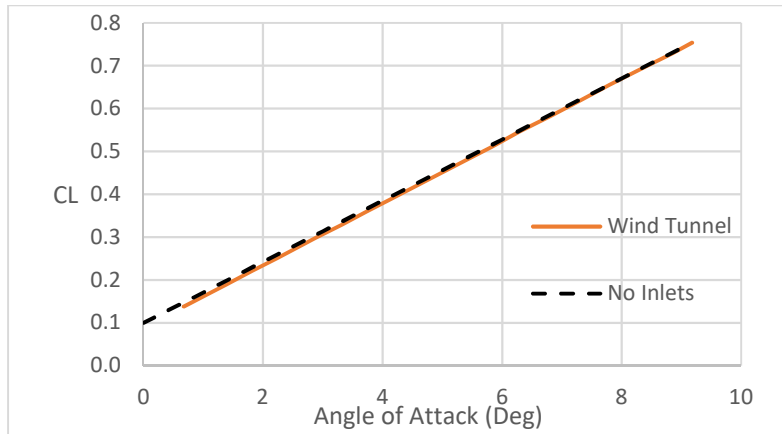


Figure 5.21: Boeing KC-135 0.077 Scale FlightStream® Analysis

After properly scaling the aircraft and entering the correct wind tunnel conditions, FlightStream® was able to generate the results shown in Figures 5.22. FlightStream® is illustrated with the dot and the wind tunnel data is illustrated with the blue line. Lateral spacing is of importance here. At zero lateral spacing, the aircraft are directly in line with each other. A lateral spacing of 0.5 is represented when the UAV nose is aligned with the tankers wing tip. A lateral spacing of 1.0 is represented when the left-wing tip of the UAV is aligned with the right-wing tip of the tanker. The remaining positions were determined from the scaling used to

establish those positions. There is no vertical spacing here. The longitudinal spacing is $x/b = 0.85$, which represents 20 feet full scale.

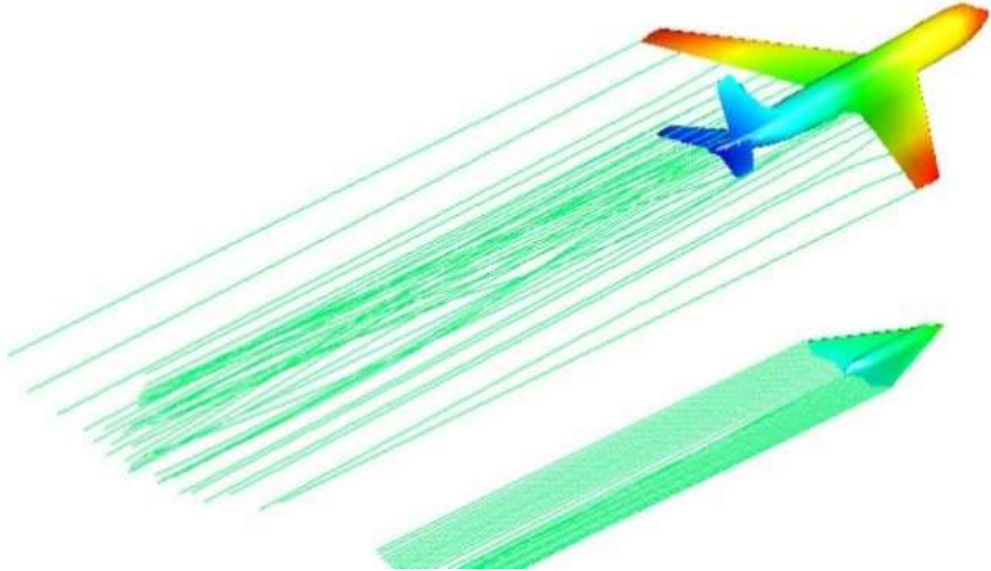
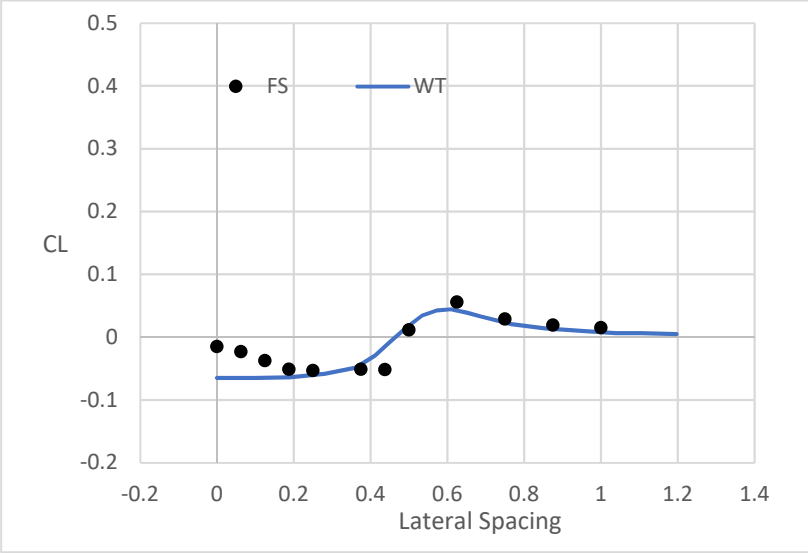


Figure 5.22: Aerial Refueling FlightStream® Analysis

Chapter 6

Concluding Remarks

6.1 Conclusion to Validation Analysis

FlightStream® accurately predicts the aerodynamic loads for a wide range of the given aircraft in the environments and flight conditions established by the wind tunnel tests.

FlightStream® successfully predicted the coefficient of lift per angle of attack for the Boeing KC-135 and ICE-Configuration UAV individually. Then FlightStream® proved to be an efficient computational tool by providing accurate solutions of the aircraft in close-proximity flight. FlightStream® correctly predicted the coefficient of lift of the trailing aircraft per lateral spacing behind the lead aircraft at given angle of attack for both a formation flight and aerial refuel.

6.2 Future Work

6.2.1 FlightStream® Updates

FlightStream® updates continue abreast and this tool appears to be on track to be the industry leader for efficient and robust analysis at the conceptual and preliminary stages of aircraft design. For example, at the conclusion of this research a recent update enables an easier method of analysis with two aircraft in the same environment at different angle of attacks. This update only enhances its capabilities in a close-proximity flight analysis. More formation flight wind tunnel data obtained can be compared with FlightStream® for further validation efforts.

Additional current development programs include boundary layer displacement, loads under separated flow (high lift) conditions, and improvements in propeller wake modeling, the addition of supersonic flow modeling, gust response modeling, and airship centric applications.

6.2.2 Commercial Sector

The concept of in-flight refueling has been used by the military but has not yet reached the commercial sector for routine use. A Commercial airliner must carry all the fuel required for the task at hand. If aerial refueling were brought to the commercial sector, this could result to a subsequent change in how airplanes are designed. Benefits include increased revenue to both manufacturers and airline operators. There will be the opportunity for more revenue flight hours and increased airframe life. With the option of payload increase and range extension, there would be an increase in the use of point-to-point flying. Not only does this concept benefit the airliner industry, but a reduction in takeoff weight would also help noise issues from larger commercial aircraft in heavily populated areas; thus, tackling another common problem in the process.⁵ Future endeavors would include aerodynamic studies with commercial airliners to gather more stability control data to enhance the design process to ensure further progression into using air-to-air refueling. On still more futuristic note, range is the limiting factor on adopting more electric aircraft. With proximity flight, recharging, battery exchange, or supplementary refueling could be a possible game changer for the adoption of more electric propulsion.

6.2.3 Boeing KC-46 Aerial Refueling Analysis

Along with future efforts to expand commercial aerial refueling, the military is seeking options to replace the Boeing KC-135 fleet with a Boeing KC-46 aircraft. The Air Force is expected to fill the slot of up to 40 percent of the Air Force's aging aerial refueling tanker fleet. This need for replacement is due to the increasing cost to maintain and support these aging aircraft. The KC-46 will essentially be a militarized Boeing 767 with a cargo door and other military systems added for threat detection. It is expected to have both the flying boom option and a permanent hose-and-drogue system to refuel receiving aircraft.²⁷ Future research efforts

would include a FlightStream® analysis to compare with the flight test data, such as done here with the KC-135 and UAV refueling scenario. With test data being available to the public, an aerodynamic analysis would be limited to qualitative considerations. FlightStream® can also be used in the early computational research stages of predicting aerodynamic loads and moments of the KC-46 as the lead aircraft in a refueling environment and how its wake affects the trailing aircraft.

Appendices

Appendix 1

KC-135 FlightStream® Analysis

Aerodynamic Loads

```
Simulation file: C:\Users\Taylor
Owens\Desktop\Thesis_Owens\KC135\KC_135_077_noinlets.fsm
Angle of attack (Deg) .000
Side-slip angle (Deg) .000
Free-stream velocity (ft/sec) 272.001
Requested solver iterations 100
Solver convergence limit 1.000E-04
Force solver to run all iterations F
Courant number 10.000
Karman-Tsien compressibility
Solver mode: Steady
Reference velocity (ft/sec) 272.000
Reference length (ft) 1.480
Reference area (ft^2) 6.275
Parallel processors 4
Prescribed wake T
Wake refinement size (% average mesh size) 300.000
Reynolds Number 1152927.
Coordinate frame for analysis: Reference
Current solver iteration number: 100
```


Surface, Cx, Cy, Cz, CL, CDi, CDo, CMx, CMy, CMz


```
FuselageGeom_Surf0 ,+0.0056 ,+0.0000 ,+0.0000 ,+0.0000 ,+0.0000 ,+0.0056
,+0.0001 , -0.0242 , -0.0068 ,
WingGeom_Surf0 ,+0.0011 , -0.0002 , -0.0000 , -0.0000 ,+0.0000 ,+0.0011
,+0.0140 ,+0.0042 , -0.1156 ,
WingGeom_Surf0 ,+0.0016 ,+0.0000 , -0.0044 , -0.0044 ,+0.0000 ,+0.0016
,+0.0031 , -0.0267 , -0.0012 ,
WingGeom_Surf0 ,+0.0097 ,+0.0000 ,+0.1031 ,+0.1031 ,+0.0006 ,+0.0090
,+0.3242 , -0.2201 , -0.0985 ,
Total ,+0.0180 , -0.0002 ,+0.0987 ,+0.0987 ,+0.0006 ,+0.0173 ,+0.3414
,-0.2668 , -0.2221 ,
```


Software : Flightstream

Aerodynamic Loads

Simulation file: C:\Users\Taylor
Owens\Desktop\Thesis_Owens\KC135\KC_135_077_noinlets.fsm
Angle of attack (Deg) 1.000
Side-slip angle (Deg) .000
Free-stream velocity (ft/sec) 272.001
Requested solver iterations 100
Solver convergence limit 1.000E-04
Force solver to run all iterations F
Courant number 10.000
Karman-Tsien compressibility
Solver mode: Steady
Reference velocity (ft/sec) 272.000
Reference length (ft) 1.480
Reference area (ft^2) 6.275
Parallel processors 4
Prescribed wake T
Wake refinement size (% average mesh size) 300.000
Reynolds Number 1152927.
Coordinate frame for analysis: Reference
Current solver iteration number: 143

Surface, Cx, Cy, Cz, CL, CDi, CDo, CMx, CMy, CMz

FuselageGeom_Surf0 ,+0.0056 ,+0.0000 ,+0.0001 ,+0.0000 ,+0.0000 ,+0.0056
,+0.0001 , -0.0275 , -0.0069 ,
WingGeom_Surf0 ,+0.0011 ,+0.0005 ,+0.0000 ,+0.0000 , -0.0000 ,+0.0011
,+0.0101 , -0.0015 , -0.0926 ,
WingGeom_Surf0 ,+0.0016 ,+0.0000 ,+0.0018 ,+0.0018 ,+0.0000 ,+0.0016
,+0.0030 , -0.0404 ,+0.0012 ,
WingGeom_Surf0 ,+0.0077 ,+0.0000 ,+0.1687 ,+0.1686 ,+0.0016 ,+0.0091
,+0.3234 , -0.3242 , -0.0982 ,
Total ,+0.0160 ,+0.0005 ,+0.1706 ,+0.1704 ,+0.0016 ,+0.0174 ,+0.3366
, -0.3936 , -0.1965 ,

Software : Flightstream

Aerodynamic Loads

```

Simulation file: C:\Users\Taylor
Owens\Desktop\Thesis_Owens\KC135\KC_135_077_noinlets.fsm
Angle of attack (Deg) 3.000
Side-slip angle (Deg) .000
Free-stream velocity (ft/sec) 272.001
Requested solver iterations 100
Solver convergence limit 1.000E-04
Force solver to run all iterations F
Courant number 10.000
Karman-Tsien compressibility
Solver mode: Steady
Reference velocity (ft/sec) 272.000
Reference length (ft) 1.480
Reference area (ft^2) 6.275
Parallel processors 4
Prescribed wake T
Wake refinement size (% average mesh size) 300.000
Reynolds Number 1152927.
Coordinate frame for analysis: Reference
Current solver iteration number: 163

```

 Surface, Cx, Cy, Cz, CL, CDi, CDo, CMx, CMy, CMz

```

-----
FuselageGeom_Surf0 ,+0.0057 ,+0.0000 ,+0.0003 ,+0.0000 ,+0.0000 ,+0.0057
,+0.0001 ,-0.0294 ,-0.0072 ,
WingGeom_Surf0 ,+0.0011 ,+0.0006 ,+0.0001 ,-0.0000 ,+0.0000 ,+0.0011
,+0.0088 ,-0.0030 ,-0.0845 ,
WingGeom_Surf0 ,+0.0013 ,+0.0001 ,+0.0081 ,+0.0080 ,+0.0001 ,+0.0016
,+0.0029 ,-0.0591 ,+0.0017 ,
WingGeom_Surf0 ,-0.0002 ,+0.0000 ,+0.2341 ,+0.2338 ,+0.0029 ,+0.0091
,+0.3222 ,-0.4254 ,-0.0980 ,
Total ,+0.0079 ,+0.0007 ,+0.2426 ,+0.2418 ,+0.0030 ,+0.0175 ,+0.3340
,-0.5169 ,-0.1880 ,
-----

```

 Software : Flightstream

Aerodynamic Loads

```

Simulation file:                C:\Users\Taylor
Owens\Desktop\Thesis_Owens\KC135\KC_135_077_noinlets.fsm
Angle of attack (Deg)           4.000
Side-slip angle (Deg)          .000
Free-stream velocity (ft/sec)  272.001
Requested solver iterations     100
Solver convergence limit       1.000E-04
Force solver to run all iterations F
Courant number                  10.000
Karman-Tsien compressibility
Solver mode:                    Steady
Reference velocity (ft/sec)    272.000
Reference length (ft)          1.480
Reference area (ft^2)          6.275
Parallel processors             4
Prescribed wake                 T
Wake refinement size (% average mesh size) 300.000
Reynolds Number                 1152927.
Coordinate frame for analysis:  Reference
Current solver iteration number: 197

```

 Surface, Cx, Cy, Cz, CL, CDi, CDo, CMx, CMy, CMz

```

FuselageGeom_Surf0 ,+0.0057 ,+0.0000 ,+0.0004 ,+0.0000 ,+0.0000 ,+0.0057
,+0.0000 ,-0.0322 ,-0.0080 ,
WingGeom_Surf0 ,+0.0011 ,+0.0007 ,+0.0001 ,-0.0000 ,+0.0000 ,+0.0011
,+0.0072 ,-0.0044 ,-0.0742 ,
WingGeom_Surf0 ,+0.0008 ,+0.0001 ,+0.0204 ,+0.0203 ,+0.0006 ,+0.0016
,+0.0025 ,-0.0976 ,+0.0025 ,
WingGeom_Surf0 ,-0.0094 ,+0.0000 ,+0.3641 ,+0.3638 ,+0.0069 ,+0.0091
,+0.3174 ,-0.6066 ,-0.0975 ,
Total ,-0.0018 ,+0.0008 ,+0.3850 ,+0.3841 ,+0.0075 ,+0.0175 ,+0.3271
,-0.7408 ,-0.1772 ,

```

 Software : Flightstream

Aerodynamic Loads

```

Simulation file:                               C:\Users\Taylor
Owens\Desktop\Thesis_Owens\KC135\KC_135_077_noinlets.fsm
Angle of attack (Deg)                          5.000
Side-slip angle (Deg)                         .000
Free-stream velocity (ft/sec)                 272.001
Requested solver iterations                   100
Solver convergence limit                     1.000E-04
Force solver to run all iterations           F
Courant number                               10.000
Karman-Tsien compressibility
Solver mode:                                  Steady
Reference velocity (ft/sec)                  272.000
Reference length (ft)                       1.480
Reference area (ft^2)                       6.275
Parallel processors                          4
Prescribed wake                              T
Wake refinement size (% average mesh size)  300.000
Reynolds Number                             1152927.
Coordinate frame for analysis:               Reference
Current solver iteration number:             216
    
```


 Surface, Cx, Cy, Cz, CL, CDi, CDo, CMx, CMy, CMz


```

FuselageGeom_Surf0 ,+0.0057 ,+0.0000 ,+0.0005 ,+0.0000 ,+0.0000 ,+0.0057
,+0.0000 ,-0.0335 ,-0.0082 ,
WingGeom_Surf0 ,+0.0011 ,+0.0008 ,+0.0001 ,+0.0000 ,-0.0000 ,+0.0011
,+0.0065 ,-0.0049 ,-0.0694 ,
WingGeom_Surf0 ,+0.0002 ,+0.0001 ,+0.0263 ,+0.0262 ,+0.0009 ,+0.0016
,+0.0031 ,-0.1156 ,+0.0019 ,
WingGeom_Surf0 ,-0.0190 ,+0.0000 ,+0.4288 ,+0.4288 ,+0.0095 ,+0.0089
,+0.3159 ,-0.7004 ,-0.0974 ,
Total ,-0.0120 ,+0.0009 ,+0.4557 ,+0.4550 ,+0.0104 ,+0.0173 ,+0.3255
,-0.8544 ,-0.1731 ,
    
```


 Software : Flightstream

Aerodynamic Loads

```
Simulation file: C:\Users\Taylor
Owens\Desktop\Thesis_Owens\KC135\KC_135_077_noinlets.fsm
Angle of attack (Deg) 6.000
Side-slip angle (Deg) .000
Free-stream velocity (ft/sec) 272.001
Requested solver iterations 100
Solver convergence limit 1.000E-04
Force solver to run all iterations F
Courant number 10.000
Karman-Tsien compressibility
Solver mode: Steady
Reference velocity (ft/sec) 272.000
Reference length (ft) 1.480
Reference area (ft^2) 6.275
Parallel processors 4
Prescribed wake T
Wake refinement size (% average mesh size) 300.000
Reynolds Number 1152927.
Coordinate frame for analysis: Reference
Current solver iteration number: 233
```


Surface, Cx, Cy, Cz, CL, CDi, CDo, CMx, CMy, CMz


```
FuselageGeom_Surf0 ,+0.0057 ,+0.0000 ,+0.0006 ,+0.0000 ,+0.0000 ,+0.0057
,+0.0000 ,-0.0346 ,-0.0086 ,
WingGeom_Surf0 ,+0.0011 ,+0.0009 ,+0.0001 ,+0.0000 ,-0.0000 ,+0.0011
,+0.0059 ,-0.0052 ,-0.0651 ,
WingGeom_Surf0 ,-0.0006 ,+0.0001 ,+0.0331 ,+0.0330 ,+0.0013 ,+0.0015
,+0.0035 ,-0.1324 ,+0.0019 ,
WingGeom_Surf0 ,-0.0304 ,+0.0000 ,+0.4932 ,+0.4937 ,+0.0126 ,+0.0088
,+0.3149 ,-0.7980 ,-0.0972 ,
Total ,-0.0242 ,+0.0010 ,+0.5270 ,+0.5267 ,+0.0139 ,+0.0171 ,+0.3243
,-0.9702 ,-0.1690 ,
```


Software : Flightstream

Aerodynamic Loads

```

Simulation file:                               C:\Users\Taylor
Owens\Desktop\Thesis_Owens\KC135\KC_135_077_noinlets.fsm
Angle of attack (Deg)                          7.000
Side-slip angle (Deg)                         .000
Free-stream velocity (ft/sec)                 272.001
Requested solver iterations                   100
Solver convergence limit                     1.000E-04
Force solver to run all iterations           F
Courant number                               10.000
Karman-Tsien compressibility
Solver mode:                                  Steady
Reference velocity (ft/sec)                  272.000
Reference length (ft)                       1.480
Reference area (ft^2)                       6.275
Parallel processors                          4
Prescribed wake                              T
Wake refinement size (% average mesh size)  300.000
Reynolds Number                             1152927.
Coordinate frame for analysis:               Reference
Current solver iteration number:             249

```


 Surface, Cx, Cy, Cz, CL, CDi, CDo, CMx, CMy, CMz


```

FuselageGeom_Surf0 ,+0.0057 ,+0.0000 ,+0.0007 ,+0.0000 ,+0.0000 ,+0.0057
,+0.0000 ,-0.0356 ,-0.0090 ,
WingGeom_Surf0 ,+0.0011 ,+0.0009 ,+0.0001 ,+0.0000 ,-0.0000 ,+0.0011
,+0.0055 ,-0.0054 ,-0.0617 ,
WingGeom_Surf0 ,-0.0015 ,+0.0000 ,+0.0393 ,+0.0392 ,+0.0019 ,+0.0014
,+0.0034 ,-0.1517 ,+0.0021 ,
WingGeom_Surf0 ,-0.0435 ,+0.0000 ,+0.5574 ,+0.5585 ,+0.0160 ,+0.0088
,+0.3134 ,-0.8962 ,-0.0969 ,
Total ,-0.0382 ,+0.0009 ,+0.5975 ,+0.5977 ,+0.0179 ,+0.0170 ,+0.3223
,-1.0889 ,-0.1655 ,

```


 Software : Flightstream

Aerodynamic Loads

Simulation file: C:\Users\Taylor
Owens\Desktop\Thesis_Owens\KC135\KC_135_077_noinlets.fsm
Angle of attack (Deg) 8.000
Side-slip angle (Deg) .000
Free-stream velocity (ft/sec) 272.001
Requested solver iterations 100
Solver convergence limit 1.000E-04
Force solver to run all iterations F
Courant number 10.000
Karman-Tsien compressibility
Solver mode: Steady
Reference velocity (ft/sec) 272.000
Reference length (ft) 1.480
Reference area (ft^2) 6.275
Parallel processors 4
Prescribed wake T
Wake refinement size (% average mesh size) 300.000
Reynolds Number 1152927.
Coordinate frame for analysis: Reference
Current solver iteration number: 264

Surface, Cx, Cy, Cz, CL, CDi, CDo, CMx, CMy, CMz

FuselageGeom_Surf0 ,+0.0057 ,+0.0000 ,+0.0008 ,+0.0000 ,+0.0000 ,+0.0058
,+0.0000 ,-0.0365 ,-0.0098 ,
WingGeom_Surf0 ,+0.0011 ,+0.0007 ,+0.0002 ,-0.0000 ,+0.0000 ,+0.0011
,+0.0052 ,-0.0055 ,-0.0597 ,
WingGeom_Surf0 ,-0.0024 ,+0.0000 ,+0.0458 ,+0.0456 ,+0.0024 ,+0.0015
,+0.0035 ,-0.1728 ,+0.0021 ,
WingGeom_Surf0 ,-0.0585 ,-0.0000 ,+0.6211 ,+0.6232 ,+0.0199 ,+0.0086
,+0.3121 ,-0.9968 ,-0.0965 ,
Total ,-0.0541 ,+0.0007 ,+0.6679 ,+0.6688 ,+0.0223 ,+0.0170 ,+0.3208
, -1.2116 ,-0.1639 ,

Software : Flightstream

Aerodynamic Loads

```

Simulation file:                C:\Users\Taylor
Owens\Desktop\Thesis_Owens\KC135\KC_135_077_noinlets.fsm
Angle of attack (Deg)           9.000
Side-slip angle (Deg)          .000
Free-stream velocity (ft/sec)  272.001
Requested solver iterations     100
Solver convergence limit       1.000E-04
Force solver to run all iterations F
Courant number                 10.000
Karman-Tsien compressibility
Solver mode:                   Steady
Reference velocity (ft/sec)    272.000
Reference length (ft)         1.480
Reference area (ft^2)         6.275
Parallel processors            4
Prescribed wake                T
Wake refinement size (% average mesh size) 300.000
Reynolds Number                1152927.
Coordinate frame for analysis: Reference
Current solver iteration number: 279

```


 Surface, Cx, Cy, Cz, CL, CDi, CDo, CMx, CMy, CMz


```

FuselageGeom_Surf0 ,+0.0057 ,+0.0000 ,+0.0009 ,+0.0000 ,+0.0000 ,+0.0058
,+0.0000 ,-0.0372 ,-0.0103 ,
WingGeom_Surf0 ,+0.0011 ,+0.0008 ,+0.0002 ,-0.0000 ,+0.0000 ,+0.0011
,+0.0048 ,-0.0056 ,-0.0570 ,
WingGeom_Surf0 ,-0.0035 ,+0.0000 ,+0.0520 ,+0.0519 ,+0.0032 ,+0.0015
,+0.0034 ,-0.1930 ,+0.0023 ,
WingGeom_Surf0 ,-0.0752 ,-0.0000 ,+0.6845 ,+0.6878 ,+0.0242 ,+0.0086
,+0.3117 ,-1.0997 ,-0.0963 ,
Total ,-0.0719 ,+0.0008 ,+0.7376 ,+0.7397 ,+0.0274 ,+0.0170 ,+0.3199
,-1.3355 ,-0.1613 ,

```


 Software : Flightstream

Appendix 2

UAV FlightStream® Analysis

Aerodynamic Loads

```
Simulation file: C:\Users\Taylor
Owens\Desktop\Thesis_Owens\UAV\ICE101UAV_13.fsm
Angle of attack (Deg) .075
Side-slip angle (Deg) .000
Free-stream velocity (ft/sec) 65.000
Requested solver iterations 100
Solver convergence limit 1.000E-04
Force solver to run all iterations F
Courant number 10.000
Karman-Tsien compressibility
Solver mode: Steady
Reference velocity (ft/sec) 65.000
Reference length (ft) 1.030
Reference area (ft^2) 62.150
Parallel processors 4
Prescribed wake T
Wake refinement size (% average mesh size) 300.000
Reynolds Number 191744.
Coordinate frame for analysis: Reference
Current solver iteration number: 368
```


Surface, Cx, Cy, Cz, CL, CDi, CDo, CMx, CMy, CMz


```
WingGeom_Surf0 ,+0.0072 , -0.0000 , +0.0096 , +0.0096 , +0.0000 , +0.0072
,-0.0112 , +0.0033 , +0.0079 ,
WingGeom_Surf1 ,+0.0000 , +0.0000 , +0.0000 , +0.0000 , +0.0000 , +0.0000
,-0.0000 , -0.0000 , -0.0000 ,
FuselageGeom_Surf0 ,+0.0034 , +0.0000 , +0.0000 , +0.0000 , +0.0000 , +0.0034
,-0.0019 , -0.0651 , -0.0005 ,
Total ,+0.0106 , +0.0000 , +0.0096 , +0.0096 , +0.0000 , +0.0106 , -0.0131
,-0.0618 , +0.0074 ,
```


Software : Flightstream

Aerodynamic Loads

```
Simulation file: C:\Users\Taylor
Owens\Desktop\Thesis_Owens\UAV\ICE101UAV_13.fsm
Angle of attack (Deg) 2.030
Side-slip angle (Deg) .000
Free-stream velocity (ft/sec) 65.000
Requested solver iterations 100
Solver convergence limit 1.000E-04
Force solver to run all iterations F
Courant number 10.000
Karman-Tsien compressibility
Solver mode: Steady
Reference velocity (ft/sec) 65.000
Reference length (ft) 1.030
Reference area (ft^2) 62.150
Parallel processors 4
Prescribed wake T
Wake refinement size (% average mesh size) 300.000
Reynolds Number 191744.
Coordinate frame for analysis: Reference
Current solver iteration number: 395
```


Surface, Cx, Cy, Cz, CL, CDi, CDo, CMx, CMy, CMz

WingGeom_Surf0 ,+0.0054 , -0.0000 ,+0.0834 ,+0.0831 ,+0.0012 ,+0.0072
, -0.0120 , -0.3181 ,+0.0070 ,
WingGeom_Surf1 ,+0.0000 ,+0.0000 ,+0.0000 ,+0.0000 ,+0.0000 ,+0.0000
, -0.0000 , -0.0000 , -0.0000 ,
FuselageGeom_Surf0 ,+0.0034 ,+0.0000 ,+0.0001 ,+0.0000 ,+0.0000 ,+0.0034
, -0.0017 , -0.1279 , -0.0011 ,
Total ,+0.0088 ,+0.0000 ,+0.0835 ,+0.0831 ,+0.0012 ,+0.0106 , -0.0137
, -0.4460 ,+0.0059 ,

Software : Flightstream

Aerodynamic Loads

```
Simulation file: C:\Users\Taylor
Owens\Desktop\Thesis_Owens\UAV\ICE101UAV_13.fsm
Angle of attack (Deg) 4.060
Side-slip angle (Deg) .000
Free-stream velocity (ft/sec) 65.000
Requested solver iterations 100
Solver convergence limit 1.000E-04
Force solver to run all iterations F
Courant number 10.000
Karman-Tsien compressibility
Solver mode: Steady
Reference velocity (ft/sec) 65.000
Reference length (ft) 1.030
Reference area (ft^2) 62.150
Parallel processors 4
Prescribed wake T
Wake refinement size (% average mesh size) 300.000
Reynolds Number 191744.
Coordinate frame for analysis: Reference
Current solver iteration number: 418
```


Surface, Cx, Cy, Cz, CL, CDi, CDo, CMx, CMy, CMz


```
WingGeom_Surf0 , -0.0002 , -0.0000 , +0.1602 , +0.1598 , +0.0042 , +0.0069
, -0.0129 , -0.6493 , +0.0039 ,
WingGeom_Surf1 , +0.0000 , +0.0000 , +0.0000 , +0.0000 , +0.0000 , +0.0000
, -0.0000 , -0.0000 , -0.0000 ,
FuselageGeom_Surf0 , +0.0034 , +0.0000 , +0.0002 , +0.0000 , +0.0000 , +0.0034
, -0.0015 , -0.1929 , -0.0019 ,
Total , +0.0032 , +0.0000 , +0.1604 , +0.1598 , +0.0042 , +0.0103 , -0.0144
, -0.8422 , +0.0020 ,
```


Software : Flightstream

Aerodynamic Loads

```
Simulation file: C:\Users\Taylor
Owens\Desktop\Thesis_Owens\UAV\ICE101UAV_13.fsm
Angle of attack (Deg) 6.015
Side-slip angle (Deg) .000
Free-stream velocity (ft/sec) 65.000
Requested solver iterations 100
Solver convergence limit 1.000E-04
Force solver to run all iterations F
Courant number 10.000
Karman-Tsien compressibility
Solver mode: Steady
Reference velocity (ft/sec) 65.000
Reference length (ft) 1.030
Reference area (ft^2) 62.150
Parallel processors 4
Prescribed wake T
Wake refinement size (% average mesh size) 300.000
Reynolds Number 191744.
Coordinate frame for analysis: Reference
Current solver iteration number: 441
```


Surface, Cx, Cy, Cz, CL, CDi, CDo, CMx, CMy, CMz


```
WingGeom_Surf0 , -0.0089 , -0.0000 , +0.2342 , +0.2339 , +0.0090 , +0.0067
, -0.0135 , -0.9651 , -0.0011 ,
WingGeom_Surf1 , +0.0000 , +0.0000 , +0.0000 , +0.0000 , +0.0000 , +0.0000
, -0.0000 , -0.0000 , -0.0000 ,
FuselageGeom_Surf0 , +0.0034 , +0.0000 , +0.0004 , +0.0000 , +0.0000 , +0.0034
, -0.0013 , -0.2552 , -0.0027 ,
Total , -0.0055 , +0.0000 , +0.2346 , +0.2339 , +0.0090 , +0.0101 , -0.0148
, -1.2203 , -0.0038 ,
```


Software : Flightstream

Aerodynamic Loads

```

Simulation file: C:\Users\Taylor
Owens\Desktop\Thesis_Owens\UAV\ICE101UAV_13.fsm
Angle of attack (Deg) 7.970
Side-slip angle (Deg) .000
Free-stream velocity (ft/sec) 65.000
Requested solver iterations 100
Solver convergence limit 1.000E-04
Force solver to run all iterations F
Courant number 10.000
Karman-Tsien compressibility
Solver mode: Steady
Reference velocity (ft/sec) 65.000
Reference length (ft) 1.030
Reference area (ft^2) 62.150
Parallel processors 4
Prescribed wake T
Wake refinement size (% average mesh size) 300.000
Reynolds Number 191744.
Coordinate frame for analysis: Reference
Current solver iteration number: 463

```

 Surface, Cx, Cy, Cz, CL, CDi, CDo, CMx, CMy, CMz

```

WingGeom_Surf0 , -0.0208 , -0.0000 , +0.3083 , +0.3082 , +0.0156 , +0.0066
, -0.0141 , -1.2766 , -0.0081 ,
WingGeom_Surf1 , +0.0000 , +0.0000 , +0.0000 , +0.0000 , +0.0000 , +0.0000
, -0.0000 , -0.0000 , -0.0000 ,
FuselageGeom_Surf0 , +0.0034 , +0.0000 , +0.0005 , +0.0000 , +0.0000 , +0.0034
, -0.0011 , -0.3171 , -0.0036 ,
Total , -0.0174 , +0.0000 , +0.3088 , +0.3082 , +0.0156 , +0.0100 , -0.0152
, -1.5937 , -0.0117 ,

```

 Software : Flightstream

Aerodynamic Loads

```
Simulation file: C:\Users\Taylor
Owens\Desktop\Thesis_Owens\UAV\ICE101UAV_13.fsm
Angle of attack (Deg) 10.000
Side-slip angle (Deg) .000
Free-stream velocity (ft/sec) 65.000
Requested solver iterations 100
Solver convergence limit 1.000E-04
Force solver to run all iterations F
Courant number 10.000
Karman-Tsien compressibility
Solver mode: Steady
Reference velocity (ft/sec) 65.000
Reference length (ft) 1.030
Reference area (ft^2) 62.150
Parallel processors 4
Prescribed wake T
Wake refinement size (% average mesh size) 300.000
Reynolds Number 191744.
Coordinate frame for analysis: Reference
Current solver iteration number: 485
```


Surface, Cx, Cy, Cz, CL, CDi, CDo, CMx, CMy, CMz


```
WingGeom_Surf0 , -0.0365 , -0.0000 , +0.3851 , +0.3856 , +0.0244 , +0.0066
, -0.0144 , -1.5948 , -0.0175 ,
WingGeom_Surf1 , +0.0000 , +0.0000 , +0.0000 , +0.0000 , +0.0000 , +0.0000
, -0.0000 , -0.0000 , -0.0000 ,
FuselageGeom_Surf0 , +0.0034 , +0.0000 , +0.0006 , +0.0000 , +0.0000 , +0.0034
, -0.0008 , -0.3807 , -0.0046 ,
Total , -0.0331 , +0.0000 , +0.3857 , +0.3856 , +0.0244 , +0.0100 , -0.0152
, -1.9755 , -0.0221 ,
```


Software : Flightstream

Aerodynamic Loads

```

Simulation file: C:\Users\Taylor
Owens\Desktop\Thesis_Owens\UAV\ICE101UAV_13.fsm
Angle of attack (Deg) 12.030
Side-slip angle (Deg) .000
Free-stream velocity (ft/sec) 65.000
Requested solver iterations 100
Solver convergence limit 1.000E-04
Force solver to run all iterations F
Courant number 10.000
Karman-Tsien compressibility
Solver mode: Steady
Reference velocity (ft/sec) 65.000
Reference length (ft) 1.030
Reference area (ft^2) 62.150
Parallel processors 4
Prescribed wake T
Wake refinement size (% average mesh size) 300.000
Reynolds Number 191744.
Coordinate frame for analysis: Reference
Current solver iteration number: 506

```


Surface, Cx, Cy, Cz, CL, CDi, CDo, CMx, CMy, CMz

```

WingGeom_Surf0 , -0.0556 , +0.0000 , +0.4617 , +0.4631 , +0.0352 , +0.0066
, -0.0145 , -1.9070 , -0.0291 ,
WingGeom_Surf1 , +0.0000 , +0.0000 , +0.0000 , +0.0000 , +0.0000 , +0.0000
, -0.0000 , -0.0000 , -0.0000 ,
FuselageGeom_Surf0 , +0.0033 , +0.0000 , +0.0007 , +0.0000 , +0.0000 , +0.0034
, -0.0005 , -0.4433 , -0.0057 ,
Total , -0.0523 , +0.0000 , +0.4624 , +0.4631 , +0.0352 , +0.0100 , -0.0150
, -2.3503 , -0.0348 ,
-----
```


Software : Flightstream

Aerodynamic Loads

```
Simulation file: C:\Users\Taylor
Owens\Desktop\Thesis_Owens\UAV\ICE101UAV_13.fsm
Angle of attack (Deg) 16.015
Side-slip angle (Deg) .000
Free-stream velocity (ft/sec) 65.000
Requested solver iterations 100
Solver convergence limit 1.000E-04
Force solver to run all iterations F
Courant number 10.000
Karman-Tsien compressibility
Solver mode: Steady
Reference velocity (ft/sec) 65.000
Reference length (ft) 1.030
Reference area (ft^2) 62.150
Parallel processors 4
Prescribed wake T
Wake refinement size (% average mesh size) 300.000
Reynolds Number 191744.
Coordinate frame for analysis: Reference
Current solver iteration number: 528
```


Surface, Cx, Cy, Cz, CL, CDi, CDo, CMx, CMy, CMz

WingGeom_Surf0 , -0.1038 , +0.0000 , +0.6110 , +0.6159 , +0.0625 , +0.0064
, -0.0140 , -2.4974 , -0.0582 ,
WingGeom_Surf1 , +0.0000 , +0.0000 , +0.0000 , +0.0000 , +0.0000 , +0.0000
, -0.0000 , -0.0000 , -0.0000 ,
FuselageGeom_Surf0 , +0.0033 , +0.0000 , +0.0009 , +0.0000 , +0.0000 , +0.0034
, +0.0000 , -0.5625 , -0.0080 ,
Total , -0.1005 , +0.0000 , +0.6119 , +0.6159 , +0.0625 , +0.0098 , -0.0140
, -3.0599 , -0.0662 ,

Software : Flightstream

Aerodynamic Loads

```

Simulation file:                               C:\Users\Taylor
Owens\Desktop\Thesis_Owens\UAV\ICE101UAV_13.fsm
Angle of attack (Deg)                          17.970
Side-slip angle (Deg)                         .000
Free-stream velocity (ft/sec)                 65.000
Requested solver iterations                   100
Solver convergence limit                     1.000E-04
Force solver to run all iterations            F
Courant number                               10.000
Karman-Tsien compressibility
Solver mode:                                  Steady
Reference velocity (ft/sec)                  65.000
Reference length (ft)                       1.030
Reference area (ft^2)                       62.150
Parallel processors                          4
Prescribed wake                              T
Wake refinement size (% average mesh size)  300.000
Reynolds Number                             191744.
Coordinate frame for analysis:               Reference
Current solver iteration number:             548

```

 Surface, Cx, Cy, Cz, CL, CDi, CDo, CMx, CMy, CMz

```

WingGeom_Surf0 , -0.1324 , +0.0000 , +0.6835 , +0.6910 , +0.0788 , +0.0062
, -0.0121 , -2.7716 , -0.0742 ,
WingGeom_Surf1 , +0.0000 , +0.0000 , +0.0000 , +0.0000 , +0.0000 , +0.0000
, -0.0000 , -0.0000 , -0.0000 ,
FuselageGeom_Surf0 , +0.0033 , +0.0000 , +0.0011 , +0.0000 , +0.0000 , +0.0034
, +0.0004 , -0.6188 , -0.0092 ,
Total , -0.1291 , +0.0000 , +0.6846 , +0.6910 , +0.0788 , +0.0096 , -0.0117
, -3.3904 , -0.0834 ,

```

 Software : Flightstream

Aerodynamic Loads

```
Simulation file: C:\Users\Taylor
Owens\Desktop\Thesis_Owens\UAV\ICE101UAV_13.fsm
Angle of attack (Deg) 20.000
Side-slip angle (Deg) .000
Free-stream velocity (ft/sec) 65.000
Requested solver iterations 100
Solver convergence limit 1.000E-04
Force solver to run all iterations F
Courant number 10.000
Karman-Tsien compressibility
Solver mode: Steady
Reference velocity (ft/sec) 65.000
Reference length (ft) 1.030
Reference area (ft^2) 62.150
Parallel processors 4
Prescribed wake T
Wake refinement size (% average mesh size) 300.000
Reynolds Number 191744.
Coordinate frame for analysis: Reference
Current solver iteration number: 568
```


Surface, Cx, Cy, Cz, CL, CDi, CDo, CMx, CMy, CMz

WingGeom_Surf0 , -0.1653 , +0.0000 , +0.7582 , +0.7691 , +0.0978 , +0.0062
, -0.0085 , -3.0419 , -0.0813 ,
WingGeom_Surf1 , +0.0000 , +0.0000 , +0.0000 , +0.0000 , +0.0000 , +0.0000
, -0.0000 , -0.0000 , -0.0000 ,
FuselageGeom_Surf0 , +0.0032 , +0.0000 , +0.0012 , +0.0000 , +0.0000 , +0.0034
, +0.0007 , -0.6752 , -0.0105 ,
Total , -0.1621 , +0.0000 , +0.7594 , +0.7691 , +0.0978 , +0.0096 , -0.0078
, -3.7171 , -0.0918 ,

Software : Flightstream

Appendix 3

UAV Formation Flight FlightStream® Analysis

Lateral Spacing: 0.5

Aerodynamic Loads

```
Simulation file: C:\Users\Taylor
Owens\Desktop\Thesis_Owens\UAV\UAV_Formation.fsm
Angle of attack (Deg) .000
Side-slip angle (Deg) .000
Free-stream velocity (ft/sec) 65.000
Requested solver iterations 100
Solver convergence limit 1.000E-04
Force solver to run all iterations F
Courant number 10.000
Karman-Tsien compressibility
Solver mode: Steady
Reference velocity (ft/sec) 65.000
Reference length (ft) 1.030
Reference area (ft^2) 62.150
Parallel processors 4
Prescribed wake F
Wake refinement size (% average mesh size) 300.000
Reynolds Number 191744.
Coordinate frame for analysis: Reference
Current solver iteration number: 92
```


Surface, Cx, Cy, Cz, CL, CDi, CDo, CMx, CMy, CMz

WingGeom_Surf0 ,+0.0253 , -0.0000 ,+0.3054 ,+0.3054 ,+0.0153 ,+0.0100
, -0.0163 , -1.6533 , -0.0101 ,
Copied surface 2 ,+0.0086 , -0.0078 , -0.0224 , -0.0224 , -0.0021 ,+0.0107
, -0.0174 , -0.5717 ,+0.2912 ,
Total ,+0.0339 , -0.0078 ,+0.2830 ,+0.2830 ,+0.0132 ,+0.0207 , -0.0337
, -2.2250 ,+0.2811 ,

Software : Flightstream

Lateral Spacing: 0.625

Aerodynamic Loads

```
Simulation file: C:\Users\Taylor
Owens\Desktop\RESEARCH\UAV\formation.fsm
Angle of attack (Deg) .000
Side-slip angle (Deg) .000
Free-stream velocity (ft/sec) 65.000
Requested solver iterations 100
Solver convergence limit 1.000E-04
Force solver to run all iterations F
Courant number 10.000
Karman-Tsien compressibility
Solver mode: Steady
Reference velocity (ft/sec) 65.000
Reference length (ft) 1.030
Reference area (ft^2) 62.150
Parallel processors 4
Prescribed wake F
Wake refinement size (% average mesh size) 300.000
Reynolds Number 191744.
Coordinate frame for analysis: Reference
Current solver iteration number: 100
```


Surface, Cx, Cy, Cz, CL, CDi, CDo, CMx, CMy, CMz


```
WingGeom_Surf0 ,+0.0253 , -0.0000 ,+0.3057 ,+0.3057 ,+0.0153 ,+0.0100
,-0.0164 , -1.6553 , -0.0102 ,
Copied surface 2 ,+0.0093 , -0.0048 ,+0.0096 ,+0.0096 , -0.0014 ,+0.0107
,-0.1323 ,+0.1432 ,+0.1700 ,
Total ,+0.0346 , -0.0048 ,+0.3153 ,+0.3153 ,+0.0139 ,+0.0207 , -0.1487
,-1.5121 ,+0.1598 ,
```


Software : Flightstream

Lateral Spacing: 0.75

Aerodynamic Loads

```
Simulation file: C:\Users\Taylor
Owens\Desktop\Thesis_Owens\UAV\UAV_Formation.fsm
Angle of attack (Deg) .000
Side-slip angle (Deg) .000
Free-stream velocity (ft/sec) 65.000
Requested solver iterations 100
Solver convergence limit 1.000E-04
Force solver to run all iterations F
Courant number 10.000
Karman-Tsien compressibility
Solver mode: Steady
Reference velocity (ft/sec) 65.000
Reference length (ft) 1.030
Reference area (ft^2) 62.150
Parallel processors 4
Prescribed wake F
Wake refinement size (% average mesh size) 300.000
Reynolds Number 191744.
Coordinate frame for analysis: Reference
Current solver iteration number: 100
```


Surface, Cx, Cy, Cz, CL, CDi, CDo, CMx, CMy, CMz

WingGeom_Surf0 ,+0.0254 , -0.0000 ,+0.3060 ,+0.3060 ,+0.0154 ,+0.0100
, -0.0164 , -1.6566 , -0.0102 ,
Copied surface 2 ,+0.0097 , -0.0015 ,+0.0333 ,+0.0333 , -0.0010 ,+0.0107
, -0.2587 ,+0.7329 ,+0.0992 ,
Total ,+0.0351 , -0.0015 ,+0.3393 ,+0.3393 ,+0.0144 ,+0.0207 , -0.2751
, -0.9237 ,+0.0890 ,

Software : Flightstream

Lateral Spacing: 0.875

Aerodynamic Loads

```
Simulation file: C:\Users\Taylor
Owens\Desktop\Thesis_Owens\UAV\UAV_Formation.fsm
Angle of attack (Deg) .000
Side-slip angle (Deg) .000
Free-stream velocity (ft/sec) 65.000
Requested solver iterations 100
Solver convergence limit 1.000E-04
Force solver to run all iterations F
Courant number 10.000
Karman-Tsien compressibility
Solver mode: Steady
Reference velocity (ft/sec) 65.000
Reference length (ft) 1.030
Reference area (ft^2) 62.150
Parallel processors 4
Prescribed wake F
Wake refinement size (% average mesh size) 300.000
Reynolds Number 191744.
Coordinate frame for analysis: Reference
Current solver iteration number: 100
```

Surface, Cx, Cy, Cz, CL, CDi, CDo, CMx, CMy, CMz

WingGeom_Surf0 ,+0.0254 , -0.0000 ,+0.3060 ,+0.3060 ,+0.0154 ,+0.0100
, -0.0164 , -1.6572 , -0.0102 ,
Copied surface 2 ,+0.0100 ,+0.0006 ,+0.0454 ,+0.0454 , -0.0007 ,+0.0107
, -0.3319 ,+0.9961 ,+0.0695 ,
Total ,+0.0354 ,+0.0006 ,+0.3514 ,+0.3514 ,+0.0147 ,+0.0207 , -0.3483
, -0.6611 ,+0.0593 ,

Software : Flightstream

Lateral Spacing: 1.0

Aerodynamic Loads

```
Simulation file: C:\Users\Taylor
Owens\Desktop\Thesis_Owens\UAV\UAV_Formation.fsm
Angle of attack (Deg) .000
Side-slip angle (Deg) .000
Free-stream velocity (ft/sec) 65.000
Requested solver iterations 100
Solver convergence limit 1.000E-04
Force solver to run all iterations F
Courant number 10.000
Karman-Tsien compressibility
Solver mode: Steady
Reference velocity (ft/sec) 65.000
Reference length (ft) 1.030
Reference area (ft^2) 62.150
Parallel processors 4
Prescribed wake F
Wake refinement size (% average mesh size) 300.000
Reynolds Number 191744.
Coordinate frame for analysis: Reference
Current solver iteration number: 100
```


Surface, Cx, Cy, Cz, CL, CDi, CDo, CMx, CMy, CMz

WingGeom_Surf0 ,+0.0254 , -0.0000 ,+0.3060 ,+0.3060 ,+0.0154 ,+0.0100
, -0.0164 , -1.6571 , -0.0102 ,
Copied surface 2 ,+0.0101 ,+0.0013 ,+0.0416 ,+0.0416 , -0.0006 ,+0.0107
, -0.3267 ,+0.8890 ,+0.0579 ,
Total ,+0.0355 ,+0.0013 ,+0.3476 ,+0.3476 ,+0.0148 ,+0.0207 , -0.3431
, -0.7681 ,+0.0477 ,

Software : Flightstream

Lateral Spacing: 1.125

Aerodynamic Loads

```
Simulation file: C:\Users\Taylor
Owens\Desktop\Thesis_Owens\UAV\UAV_Formation.fsm
Angle of attack (Deg) .000
Side-slip angle (Deg) .000
Free-stream velocity (ft/sec) 65.000
Requested solver iterations 100
Solver convergence limit 1.000E-04
Force solver to run all iterations F
Courant number 10.000
Karman-Tsien compressibility
Solver mode: Steady
Reference velocity (ft/sec) 65.000
Reference length (ft) 1.030
Reference area (ft^2) 62.150
Parallel processors 4
Prescribed wake F
Wake refinement size (% average mesh size) 300.000
Reynolds Number 191744.
Coordinate frame for analysis: Reference
Current solver iteration number: 100
```


Surface, Cx, Cy, Cz, CL, CDi, CDo, CMx, CMy, CMz

WingGeom_Surf0 ,+0.0254 , -0.0000 ,+0.3059 ,+0.3059 ,+0.0154 ,+0.0100
, -0.0164 , -1.6568 , -0.0102 ,
Copied surface 2 ,+0.0103 ,+0.0009 ,+0.0328 ,+0.0328 , -0.0003 ,+0.0107
, -0.2922 ,+0.6952 ,+0.0604 ,
Total ,+0.0357 ,+0.0009 ,+0.3387 ,+0.3387 ,+0.0151 ,+0.0207 , -0.3086
, -0.9616 ,+0.0502 ,

Software : Flightstream

Lateral Spacing: 1.25

Aerodynamic Loads

```
Simulation file: C:\Users\Taylor
Owens\Desktop\Thesis_Owens\UAV\UAV_Formation.fsm
Angle of attack (Deg) .000
Side-slip angle (Deg) .000
Free-stream velocity (ft/sec) 65.000
Requested solver iterations 100
Solver convergence limit 1.000E-04
Force solver to run all iterations F
Courant number 10.000
Karman-Tsien compressibility
Solver mode: Steady
Reference velocity (ft/sec) 65.000
Reference length (ft) 1.030
Reference area (ft^2) 62.150
Parallel processors 4
Prescribed wake F
Wake refinement size (% average mesh size) 300.000
Reynolds Number 191744.
Coordinate frame for analysis: Reference
Current solver iteration number: 100
```


Surface, Cx, Cy, Cz, CL, CDi, CDo, CMx, CMy, CMz

WingGeom_Surf0 ,+0.0254 , -0.0000 , +0.3059 , +0.3059 , +0.0154 , +0.0100
, -0.0164 , -1.6566 , -0.0102 ,
Copied surface 2 , +0.0105 , +0.0005 , +0.0245 , +0.0245 , -0.0002 , +0.0106
, -0.2543 , +0.5093 , +0.0685 ,
Total , +0.0359 , +0.0005 , +0.3304 , +0.3304 , +0.0152 , +0.0206 , -0.2707
, -1.1473 , +0.0583 ,

Software : Flightstream

Appendix 4

Aerial Refueling FlightStream® Analysis

Lateral Spacing: 0.0

Aerodynamic Loads

```
Simulation file: C:\Users\Taylor
Owens\Desktop\Thesis_Owens\WIP.fsm
Angle of attack (Deg) .000
Side-slip angle (Deg) .000
Free-stream velocity (ft/sec) 65.000
Requested solver iterations 100
Solver convergence limit 1.000E-04
Force solver to run all iterations F
Courant number 10.000
Karman-Tsien compressibility
Solver mode: Steady
Reference velocity (ft/sec) 65.000
Reference length (ft) 1.030
Reference area (ft^2) 62.200
Parallel processors 4
Prescribed wake F
Wake refinement size (% average mesh size) 300.000
Reynolds Number 197620.
Coordinate frame for analysis: Reference
Current solver iteration number: 77
```


Surface, Cx, Cy, Cz, CL, CDi, CDo, CMx, CMy, CMz

KC135 ,+0.0675 , -0.0010 ,+0.7199 ,+0.7199 ,+0.0180 ,+0.0495 ,+7.8919
, -12.7165 , -5.9324 ,
UAV ,+0.0100 ,+0.0010 , -0.0147 , -0.0147 , -0.0007 ,+0.0107 , -0.0229
, +0.4082 ,+0.1001 ,
Total ,+0.0775 ,+0.0000 ,+0.7052 ,+0.7052 ,+0.0173 ,+0.0602 ,+7.8690
, -12.3083 , -5.8323 ,

Software : Flightstream

Lateral Spacing: 0.0625

Aerodynamic Loads

```
Simulation file: C:\Users\Taylor
Owens\Desktop\Thesis_Owens\WIP.fsm
Angle of attack (Deg) .000
Side-slip angle (Deg) .000
Free-stream velocity (ft/sec) 65.000
Requested solver iterations 100
Solver convergence limit 1.000E-04
Force solver to run all iterations F
Courant number 10.000
Karman-Tsien compressibility
Solver mode: Steady
Reference velocity (ft/sec) 65.000
Reference length (ft) 1.030
Reference area (ft^2) 62.200
Parallel processors 4
Prescribed wake F
Wake refinement size (% average mesh size) 300.000
Reynolds Number 197620.
Coordinate frame for analysis: Reference
Current solver iteration number: 100
```


Surface, Cx, Cy, Cz, CL, CDi, CDo, CMx, CMy, CMz

KC135 ,+0.0678 ,+0.0004 ,+0.7199 ,+0.7199 ,+0.0180 ,+0.0497 ,+7.8709
, -12.7192 , -5.7369 ,
UAV ,+0.0098 ,+0.0035 , -0.0228 , -0.0228 , -0.0008 ,+0.0106 , -0.0842
, +0.7160 ,+0.1619 ,
Total ,+0.0776 ,+0.0039 ,+0.6971 ,+0.6971 ,+0.0172 ,+0.0603 ,+7.7867
, -12.0032 , -5.5750 ,

Software : Flightstream

Lateral Spacing: 0.125

Aerodynamic Loads

```
Simulation file: C:\Users\Taylor
Owens\Desktop\Thesis_Owens\WIP.fsm
Angle of attack (Deg) .000
Side-slip angle (Deg) .000
Free-stream velocity (ft/sec) 65.000
Requested solver iterations 100
Solver convergence limit 1.000E-04
Force solver to run all iterations F
Courant number 10.000
Karman-Tsien compressibility
Solver mode: Steady
Reference velocity (ft/sec) 65.000
Reference length (ft) 1.030
Reference area (ft^2) 62.200
Parallel processors 4
Prescribed wake F
Wake refinement size (% average mesh size) 300.000
Reynolds Number 197620.
Coordinate frame for analysis: Reference
Current solver iteration number: 100
```


Surface, Cx, Cy, Cz, CL, CDi, CDo, CMx, CMy, CMz

KC135 ,+0.0677 ,+0.0003 ,+0.7194 ,+0.7194 ,+0.0180 ,+0.0497 ,+7.8713
, -12.7118 , -5.7443 ,
UAV ,+0.0095 ,+0.0018 , -0.0373 , -0.0373 , -0.0010 ,+0.0105 , -0.1670
, +1.2446 ,+0.0495 ,
Total ,+0.0772 ,+0.0021 ,+0.6821 ,+0.6821 ,+0.0170 ,+0.0602 ,+7.7043
, -11.4672 , -5.6948 ,

Software : Flightstream

Lateral Spacing: 0.1875

Aerodynamic Loads

```
Simulation file: C:\Users\Taylor
Owens\Desktop\Thesis_Owens\WIP.fsm
Angle of attack (Deg) .000
Side-slip angle (Deg) .000
Free-stream velocity (ft/sec) 65.000
Requested solver iterations 100
Solver convergence limit 1.000E-04
Force solver to run all iterations F
Courant number 10.000
Karman-Tsien compressibility
Solver mode: Steady
Reference velocity (ft/sec) 65.000
Reference length (ft) 1.030
Reference area (ft^2) 62.200
Parallel processors 4
Prescribed wake F
Wake refinement size (% average mesh size) 300.000
Reynolds Number 197620.
Coordinate frame for analysis: Reference
Current solver iteration number: 83
```


Surface, Cx, Cy, Cz, CL, CDi, CDo, CMx, CMy, CMz


```
KC135 ,+0.0675 , -0.0008 ,+0.7186 ,+0.7186 ,+0.0179 ,+0.0495 ,+7.8884
,-12.6951 , -5.9011 ,
UAV ,+0.0094 , -0.0004 , -0.0513 , -0.0513 , -0.0011 ,+0.0105 , -0.2545
,+1.7975 , -0.1111 ,
Total ,+0.0769 , -0.0012 ,+0.6673 ,+0.6673 ,+0.0168 ,+0.0600 ,+7.6339
,-10.8976 , -6.0122 ,
```


Software : Flightstream

Lateral Spacing: 0.25

Aerodynamic Loads

```
Simulation file: C:\Users\Taylor
Owens\Desktop\Thesis_Owens\WIP.fsm
Angle of attack (Deg) .000
Side-slip angle (Deg) .000
Free-stream velocity (ft/sec) 65.000
Requested solver iterations 100
Solver convergence limit 1.000E-04
Force solver to run all iterations F
Courant number 10.000
Karman-Tsien compressibility
Solver mode: Steady
Reference velocity (ft/sec) 65.000
Reference length (ft) 1.030
Reference area (ft^2) 62.200
Parallel processors 4
Prescribed wake F
Wake refinement size (% average mesh size) 300.000
Reynolds Number 197620.
Coordinate frame for analysis: Reference
Current solver iteration number: 100
```


Surface, Cx, Cy, Cz, CL, CDi, CDo, CMx, CMy, CMz

KC135 ,+0.0677 ,+0.0003 ,+0.7195 ,+0.7195 ,+0.0180 ,+0.0497 ,+7.8714
, -12.7151 , -5.7452 ,
UAV ,+0.0096 ,+0.0004 , -0.0529 , -0.0529 , -0.0009 ,+0.0105 , -0.3620
, +1.8332 , -0.1126 ,
Total ,+0.0773 ,+0.0007 ,+0.6666 ,+0.6666 ,+0.0171 ,+0.0602 ,+7.5094
, -10.8819 , -5.8578 ,

Software : Flightstream

Lateral Spacing: 0.4

Aerodynamic Loads

```
Simulation file: C:\Users\Taylor
Owens\Desktop\Thesis_Owens\WIP.fsm
Angle of attack (Deg) .000
Side-slip angle (Deg) .000
Free-stream velocity (ft/sec) 65.000
Requested solver iterations 100
Solver convergence limit 1.000E-04
Force solver to run all iterations F
Courant number 10.000
Karman-Tsien compressibility
Solver mode: Steady
Reference velocity (ft/sec) 65.000
Reference length (ft) 1.030
Reference area (ft^2) 62.200
Parallel processors 4
Prescribed wake F
Wake refinement size (% average mesh size) 300.000
Reynolds Number 197620.
Coordinate frame for analysis: Reference
Current solver iteration number: 0
```


Surface, Cx, Cy, Cz, CL, CDi, CDo, CMx, CMy, CMz

KC135 ,+0.0677 , -0.0002 ,+0.7191 ,+0.7191 ,+0.0180 ,+0.0498 ,+7.8675
, -12.7643 , -5.6386 ,
UAV ,+0.0094 ,+0.0000 , -0.0518 , -0.0518 , -0.0011 ,+0.0106 , -0.5038
, +1.7321 , -0.1555 ,
Total ,+0.0771 , -0.0002 ,+0.6673 ,+0.6673 ,+0.0169 ,+0.0604 ,+7.3637
, -11.0322 , -5.7941 ,

Software : Flightstream

Lateral Spacing: 0.4375

Aerodynamic Loads

```
Simulation file: C:\Users\Taylor
Owens\Desktop\Thesis_Owens\WIP.fsm
Angle of attack (Deg) .000
Side-slip angle (Deg) .000
Free-stream velocity (ft/sec) 65.000
Requested solver iterations 100
Solver convergence limit 1.000E-04
Force solver to run all iterations F
Courant number 10.000
Karman-Tsien compressibility
Solver mode: Steady
Reference velocity (ft/sec) 65.000
Reference length (ft) 1.030
Reference area (ft^2) 62.200
Parallel processors 4
Prescribed wake F
Wake refinement size (% average mesh size) 300.000
Reynolds Number 197620.
Coordinate frame for analysis: Reference
Current solver iteration number: 100
```


Surface, Cx, Cy, Cz, CL, CDi, CDo, CMx, CMy, CMz


```
KC135 ,+0.0677 , -0.0002 ,+0.7191 ,+0.7191 ,+0.0180 ,+0.0498 ,+7.8674
,-12.7647 , -5.6387 ,
UAV ,+0.0094 ,+0.0000 , -0.0518 , -0.0518 , -0.0011 ,+0.0106 , -0.5038
,+1.7322 , -0.1555 ,
Total ,+0.0771 , -0.0002 ,+0.6673 ,+0.6673 ,+0.0169 ,+0.0604 ,+7.3636
,-11.0325 , -5.7942 ,
```


Software : Flightstream

Lateral Spacing: 0.5

Aerodynamic Loads

```
Simulation file: C:\Users\Taylor
Owens\Desktop\Thesis_Owens\WIP.fsm
Angle of attack (Deg) .000
Side-slip angle (Deg) .000
Free-stream velocity (ft/sec) 65.000
Requested solver iterations 100
Solver convergence limit 1.000E-04
Force solver to run all iterations F
Courant number 10.000
Karman-Tsien compressibility
Solver mode: Steady
Reference velocity (ft/sec) 65.000
Reference length (ft) 1.030
Reference area (ft^2) 62.200
Parallel processors 4
Prescribed wake F
Wake refinement size (% average mesh size) 300.000
Reynolds Number 197620.
Coordinate frame for analysis: Reference
Current solver iteration number: 100
```

Surface, Cx, Cy, Cz, CL, CDi, CDo, CMx, CMy, CMz

```
-----  
KC135 ,+0.0677 ,+0.0029 ,+0.7181 ,+0.7181 ,+0.0179 ,+0.0497 ,+7.8582  
, -12.6332 , -5.6264 ,  
UAV ,+0.0102 , -0.0031 ,+0.0117 ,+0.0117 , -0.0003 ,+0.0106 ,+0.2828  
, -0.6365 , -0.3989 ,  
Total ,+0.0779 , -0.0002 ,+0.7298 ,+0.7298 ,+0.0176 ,+0.0603 ,+8.1410  
, -13.2697 , -6.0253 ,  
-----
```

Software : Flightstream

Lateral Spacing: 0.625

Aerodynamic Loads

```
Simulation file: C:\Users\Taylor
Owens\Desktop\Thesis_Owens\WIP.fsm
Angle of attack (Deg) .000
Side-slip angle (Deg) .000
Free-stream velocity (ft/sec) 65.000
Requested solver iterations 100
Solver convergence limit 1.000E-04
Force solver to run all iterations F
Courant number 10.000
Karman-Tsien compressibility
Solver mode: Steady
Reference velocity (ft/sec) 65.000
Reference length (ft) 1.030
Reference area (ft^2) 62.200
Parallel processors 4
Prescribed wake F
Wake refinement size (% average mesh size) 300.000
Reynolds Number 197620.
Coordinate frame for analysis: Reference
Current solver iteration number: 100
```


Surface, Cx, Cy, Cz, CL, CDi, CDo, CMx, CMy, CMz

```
-----  
-----  
KC135 ,+0.0676 ,+0.0019 ,+0.7182 ,+0.7182 ,+0.0179 ,+0.0498 ,+7.8509  
, -12.6908 , -5.4455 ,  
UAV ,+0.0095 ,+0.0015 ,+0.0567 ,+0.0567 , -0.0011 ,+0.0105 ,+1.0660  
, -2.3206 , -0.2706 ,  
Total ,+0.0771 ,+0.0034 ,+0.7749 ,+0.7749 ,+0.0168 ,+0.0603 ,+8.9169  
, -15.0114 , -5.7161 ,  
-----
```


Software : Flightstream

Lateral Spacing: 0.75

Aerodynamic Loads

```
Simulation file: C:\Users\Taylor
Owens\Desktop\Thesis_Owens\WIP.fsm
Angle of attack (Deg) .000
Side-slip angle (Deg) .000
Free-stream velocity (ft/sec) 65.000
Requested solver iterations 100
Solver convergence limit 1.000E-04
Force solver to run all iterations F
Courant number 10.000
Karman-Tsien compressibility
Solver mode: Steady
Reference velocity (ft/sec) 65.000
Reference length (ft) 1.030
Reference area (ft^2) 62.200
Parallel processors 4
Prescribed wake F
Wake refinement size (% average mesh size) 300.000
Reynolds Number 197620.
Coordinate frame for analysis: Reference
Current solver iteration number: 100
```


Surface, Cx, Cy, Cz, CL, CDi, CDo, CMx, CMy, CMz


```
KC135 ,+0.0676 ,+0.0018 ,+0.7174 ,+0.7174 ,+0.0178 ,+0.0498 ,+7.8503
,-12.6779 ,-5.4486 ,
UAV ,+0.0104 ,+0.0006 ,+0.0290 ,+0.0290 ,-0.0002 ,+0.0106 ,+0.6923
,-1.2648 ,-0.4379 ,
Total ,+0.0780 ,+0.0024 ,+0.7464 ,+0.7464 ,+0.0176 ,+0.0604 ,+8.5426
,-13.9427 ,-5.8865 ,
```


Software : Flightstream

Lateral Spacing: 0.875

Aerodynamic Loads

```
Simulation file: C:\Users\Taylor
Owens\Desktop\Thesis_Owens\WIP.fsm
Angle of attack (Deg) .000
Side-slip angle (Deg) .000
Free-stream velocity (ft/sec) 65.000
Requested solver iterations 100
Solver convergence limit 1.000E-04
Force solver to run all iterations F
Courant number 10.000
Karman-Tsien compressibility
Solver mode: Steady
Reference velocity (ft/sec) 65.000
Reference length (ft) 1.030
Reference area (ft^2) 62.200
Parallel processors 4
Prescribed wake F
Wake refinement size (% average mesh size) 300.000
Reynolds Number 197620.
Coordinate frame for analysis: Reference
Current solver iteration number: 100
```


Surface, Cx, Cy, Cz, CL, CDi, CDo, CMx, CMy, CMz

KC135 ,+0.0678 , -0.0001 , +0.7202 , +0.7202 , +0.0181 , +0.0498 , +7.8711
, -12.7721 , -5.6477 ,
UAV ,+0.0105 , +0.0003 , +0.0192 , +0.0192 , -0.0000 , +0.0106 , +0.5750
, -0.8915 , -0.5297 ,
Total ,+0.0783 , +0.0002 , +0.7394 , +0.7394 , +0.0181 , +0.0604 , +8.4461
, -13.6636 , -6.1774 ,

Software : Flightstream

Lateral Spacing: 1.0

Aerodynamic Loads

```
Simulation file: C:\Users\Taylor
Owens\Desktop\Thesis_Owens\WIP.fsm
Angle of attack (Deg) .000
Side-slip angle (Deg) .000
Free-stream velocity (ft/sec) 65.000
Requested solver iterations 100
Solver convergence limit 1.000E-04
Force solver to run all iterations F
Courant number 10.000
Karman-Tsien compressibility
Solver mode: Steady
Reference velocity (ft/sec) 65.000
Reference length (ft) 1.030
Reference area (ft^2) 62.200
Parallel processors 4
Prescribed wake F
Wake refinement size (% average mesh size) 300.000
Reynolds Number 197620.
Coordinate frame for analysis: Reference
Current solver iteration number: 100
```


Surface, Cx, Cy, Cz, CL, CDi, CDo, CMx, CMy, CMz

KC135 ,+0.0680 , -0.0005 ,+0.7221 ,+0.7221 ,+0.0182 ,+0.0497 ,+7.8798
, -12.7735 , -5.7836 ,
UAV ,+0.0106 ,+0.0001 ,+0.0149 ,+0.0149 , -0.0000 ,+0.0106 ,+0.5399
, -0.7288 , -0.6139 ,
Total ,+0.0786 , -0.0004 ,+0.7370 ,+0.7370 ,+0.0182 ,+0.0603 ,+8.4197
, -13.5023 , -6.3975 ,

Software : Flightstream

References

1. Ahuja, Vivek, and Roy Hartfield. *Aerial Refueling Tanker and Receiver Aerodynamic Interaction Modeling and Simulation Using FlightStream*.
2. Angash, Zafar & Ahmed, Anwar & Khan, Javed & P. Sanchez, Robin. (2006). Aerodynamics of Formation Flight. *Journal of Aircraft - J AIRCRAFT*. 43. 907-912. 10.2514/1.13872.
3. "Home." *U.S. Air Force*, www.af.mil/News/Photos/igphoto/2001949945/.
4. Nangia, R. K., "Operations and aircraft design towards greener civil aviation using air-to-air refuelling," *The Aeronautical Journal*, vol. 110, Apr. 2006, pp. 705–721.
5. *50 Years of Probe and Drogue Flight Refuelling Cover Signed Air Chief Marshal Sir Michael Knight KCB AFC FRAES*, www.the-best-of-british.com/PlaneCrazyHeritage/airpictorial/1999/RefuellingFDC.htm.
6. "Aerial Refueling." *Wikipedia*, Wikimedia Foundation, 10 June 2019, en.wikipedia.org/wiki/Aerial_refueling.
7. Bolkom, C., "Air Force Aerial Refueling Methods: Flying Boom versus Hose-and-Drogue," *Congressional Research Service The Library of Congress 101*, Jun. 2006.
8. Dickes, E. G., Gingras, D. R., Hultbertg, R. S., and Kloc, S. J., "Unmanned Combat Air Vehicle (UCAV) Automated Refueling Simulation Development. Delivery Order 0009: Volume 2 - KC-135," Jan. 2002. 33
9. Bolkom, Christopher. *Air Force Aerial Refueling*. 20 Mar. 2007, fas.org/sgp/crs/weapons/RS20941.pdf.

10. "Defense, Space & Security: KC-135 Stratotanker," *Boeing: Global Services & Support - MM&U - KC-135 Stratotanker Home* Available:
<https://web.archive.org/web/20110629014517/http://www.boeing.com/defense-space/military/kc135-strat/index.html>.
11. Pike, J., "KC-135R Stratotanker," *Global Security* Available:
<https://www.globalsecurity.org/military/systems/aircraft/kc-135r-mprsp.htm>.
12. "KC-135 Stratotanker," *U.S. Air Force* Available: <http://www.af.mil/About-Us/Fact-Sheets/Display/Article/104524/kc-135-stratotanker/>.
13. "KC-135 Stratotanker Historical Snapshot," *Boeing* Available:
<http://www.boeing.com/history/products/kc-135-stratotanker.page>.
14. "BOEING KC-135 STRATOTANKER." *Flight Manuals*, www.flight-manuals-online.com/product/boeing-kc-135-stratotanker/.
15. "FlightStream Unstructured Surface Vorticity Solver," *OpenVSP* Available:
http://openvsp.org/wiki/lib/exe/fetch.php?media=workshopv3:vsp_workshop_2014.pdf.
16. Gillard, William J. "Innovative Control Effectors Dynamic Wind Tunnel Test Report." <https://apps.dtic.mil/Dtic/Tr/Fulltext/u2/a362903.Pdf>, July 1998.
17. Filippone, Antonio. (2009). Inverted Jet Spoilers for Aerodynamic Control. *Journal of Aircraft - J AIRCRAFT*. 46. 1240-1252. 10.2514/1.40321.
18. Ahuja, V., "Aerodynamic Loads Over Arbitrary Bodies By Method of Integrated Circulation," 2013.
19. "FlightStream Characteristics." *Research In Flight*, 1.
<https://nari.arc.nasa.gov/sites/default/files/attachments/37FlightStream Flow Solver-VSPworkshop 2016-2.pdf>.

20. *FlightStream 2018 Capabilities*. Research In Flight, 2018, Researchinflight.com.
21. King, L., “Aerodynamic Optimization of Integrated Wing-Engine Geometry Using an Unstructured Vorticity Solver,” thesis, 2015.
22. Bennington, M. A., and Visser, K. D., “Aerial Refueling Implications for Commercial Aviation,” *Journal of Aircraft*, vol. 42, 2005, pp. 366–375.
23. *Comparison of Predicted and Measured Formation Flight*
 ...www.researchgate.net/publication/269063179_Comparison_of_Predicted_and_Measured_Formation_Flight_Interference_Effects.
24. *An Equivalent Model for UAV Automated Aerial Refueling*
 ...www.researchgate.net/publication/268556484_An_Equivalent_Model_for_UAV_Automated_Aerial_Refueling_Research.
25. “DTIC ADA419949: UAV Aerial Refueling - Wind Tunnel Results and Comparison with Analytical Predictions: Defense Technical Information Center: Free Download, Borrow, and Streaming.” *Internet Archive*, 1 Jan. 2004,
archive.org/details/DTIC_ADA419949.
26. Ishimitsu. “Design and Analysis of Winglets for Military Aircraft. Phase 2.” *Apps.dtic.mil*, apps.dtic.mil/docs/citations/ADA046152.
27. Bolkom, C., “Air Force Aerial Refueling Methods: Flying Boom versus Hose-and-Drogue,” *Congressional Research Service The Library of Congress 101*, Jun. 2006.
28. Hartfield R., and Ahuja V., and Chakraborty I., 2018 “*Aero-Propulsive Flight Mechanics for Twenty First Century Aircraft*”, in International Symposium on Sustainable Aviation 2018, Kiev, Ukraine, 2018.

29. Sobrinho, Antonio. *On the Generation of Quadrilateral Element Meshes for General CAD Surfaces*. Sept. 1996, dspace.mit.edu/bitstream/handle/1721.1/38177/36399255-MIT.pdf?sequence=2.
30. Friedman, Alex. *An Approach to Incorporate Additive Manufacturing and Rapid Prototype Testing for Aircraft Conceptual Design to Improve MDO Effectiveness*. 1 May 2015, pdfs.semanticscholar.org/6ce0/e793df678cfd0b956d438fde43871b8fca6c.pdf.